

Study the Effect of Graphite and Nano Carbon on Corrosion and Spalling resistance of the Zirconia- Graphite Refractory

A THESIS SUBMITTED IN PARTIAL FULFILLMENT
OF THE REQUIREMENT FOR THE DEGREE OF

MASTER OF TECHNOLOGY

In

Ceramic Engineering

By

GAURAV KUMAR GUGLIANI

211CR1041



**DEPARTMENT OF CERAMIC ENGINEERING
NATIONAL INSTITUTE OF TECHNOLOGY, ROURKELA
MAY 2013**

Study the Effect of Graphite and Nano Carbon on Corrosion and Spalling resistance of the Zirconia- Graphite Refractory

A THESIS SUBMITTED IN PARTIAL FULFILLMENT
OF THE REQUIREMENT FOR THE DEGREE OF

MASTER OF TECHNOLOGY

In

Ceramic Engineering

By

GAURAV KUMAR GUGLIANI

Under the Guidance

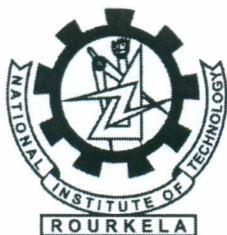
of

Prof Sumit Kumar Pal

Mr. Birendra Prasad (OCL India Ltd)



**DEPARTMENT OF CERAMIC ENGINEERING
NATIONAL INSTITUTE OF TECHNOLOGY, ROURKELA
MAY 2013**



**Department of Ceramic Engineering
National Institute of Technology,
Rourkela**



Odisha-769008

CERTIFICATE

This is to certify that the thesis entitled “Study the Effect of Graphite and Nano Carbon on Corrosion and Spalling resistance of the Zirconia-Graphite Refractory” submitted by Mr. Gaurav Kumar Gugliani to the National Institute of Technology, Rourkela in partial fulfilment of the requirements for the award of the degree of Master of Technology in Ceramic Engineering is a record of bonafide research work carried out by him under our supervision and guidance. His thesis, in our opinion, is worthy of consideration for the award of degree of Master of Technology in accordance with the regulations of the institute.

The results embodied in this thesis have not been submitted to any other university or institute for the award of a Degree.

Supervisor
Mr. Birendra Prasad
OCL India Ltd
Rajgangpur
Date: 31-05-2013

Supervisor
Dr. Sumit Kumar Pal
Department of Ceramic Engineering
National Institute of Technology
Rourkela
Date: 31-05-2013

ACKNOWLEDGEMENT

First of all, I would like to thank and deepest regard to my supervisor **Prof. Sumit Kumar Pal** Department of Ceramic Engineering, National Institute of Technology, Rourkela to always be my mentor, and **Mr. Birendra Prasad** OCL India Ltd, Rajgangpur for their guidance and continuous support

I take this great opportunity to express my gratitude and ineptness towards **Mr Anupal Sen** (OCL India Limited) and **Mr Bashir Mohammad** ((OCL India Limited)) for giving me to an opportunity to work at OCL India Limited, Rajgangpur and providing me the necessary facilities.

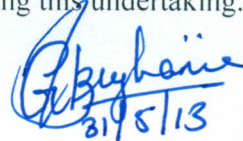
I am thankful to Prof. Swadesh Pratihar (Head of the Department) to for his valuable suggestions and help.

I am also thankful to Prof. J. Behera, Prof. S. Bhattacharya, Prof. R. Sarkar, Prof. B.B. Nayak, Prof. D. Sarkar, Prof. R. Mazumder, Prof. S. Behera, Prof. Sudip Das Gupta, Prof. Sunipa Bhattacharya and Prof. A. Chowdhury for their suggestions and support.

I am also thankful to all the technology staffs of OCL India, Limited, Rajgangpur for their cooperation throughout the work

I want to express thank to my friends R.R. Ezhil Venuswaran, Dhal Bhaiya, Mandvi Saxena, Mausam Bag, Sharad Bhaiya, Subrat Bhaiya, Ganesh Bhaiya, Sanjay Swain, and all the PhD scholars for theirs continuous support.

Last but not least, my sincere thanks to all my Mom and Dad and family members and friends who have patiently extended all sorts of help for accomplishing this undertaking.



21/5/13

GAURAV KUMAR GUGLIANI

TABLE OF CONTENTS

Certificate		i
Acknowledgement		ii
List of Content		iii
List of figures		v
List of tables		viii
Abstract		x
Chapter 1	Introduction	1
Chapter 2	Literature Review	3
	2.1 Continuous casting	3
	2.2 Necessity of sub entry nozzle	4
	2.3 Sub entry nozzle	4
	2.4 Function of sub entry nozzle	4
	2.5 Parts of sub entry nozzle	5
	2.6 Slag band of sub entry nozzle	7
	2.7 Role of Nano materials in the development of Refractories	13
Chapter 3	Objective	16
Chapter 4	Experimental procedure	17
	4.1 Raw materials	17
	4.2 Fabrication of zirconia graphite refractory	20
	4.3 General characterisation	29

Chapter 5	Results and Discussions	34
5.1	The effect of fixed carbon(FC) percentage of graphite on zirconia graphite refractory	34
5.2	Batch formulation of amorphous carbon black on zirconia graphite refractory	42
5.3	Batch formulation of zirconia graphite refractory by decreasing the graphite % and inclusion of nanocarbon	49
5.4	Batch formulation of increase in the percentage of nanocarbon on 9 wt% graphite in zirconia graphite refractory	62
Chapter 6	Conclusions	66
	References	67

LIST OF FIGURES

Fig 2.1	Schematic diagram of submerged entry nozzle	3
Fig 2.2	Parts of sub entry nozzle	5
Fig 2.3	Heat transfer from hot surface to cool surface	8
Fig 4.1	Bar showing compression height after aging	25
Fig 4.2(a)	Mold after filling the raw material	25
Fig 4.2(b)	Vibration pressing during mold filling up	25
Fig 4.3(a)	Cold isostatic pressing machine	26
Fig 4.3(b)	Cold Isostatic Pressing schedule	26
Fig 4.4	Curing furnace	27
Fig 4.5(a)	Bell cranked furnace	28
Fig 4.5(b)	Coking schedule	28
Fig 4.6	Rotary drum testing machine	32
Fig 5.1	Thermal expansion behaviour as a function of fixed carbon	36
Fig 5.2	XRD pattern of zirconia graphite refractory with 80% fixed carbon graphite, 94% FC graphite and 80% FC graphite	37
Fig 5.3	Apparent porosity as a function of fixed carbon	37
Fig 5.4	Bulk density as a function of fixed carbon	38
Fig 5.5	Cold modulus of rupture as a function of fixed carbon	39
Fig 5.6	Slag corrosion resistance as a function of fixed carbon	39
Fig 5.7	Scanning electron microscope image of (a) 99% Fixed carbon graphite (b) 94% Fixed carbon graphite (c) 80% fixed carbon graphite in zirconia graphite refractory	41
Fig 5.8	Thermal expansion behaviour as a function of 94% fixed carbon graphite with ACB	43

Fig 5.9	XRD pattern for 94% graphite with ACB and 94% without ACB	44
Fig 5.10	Apparent porosity as function of amorphous carbon black	45
Fig 5.11	Bulk density as a function of amorphous carbon black	46
Fig 5.12	Cold modulus of rupture as a function of amorphous carbon black	47
Fig 5.13	Variation of width loss caused by the slag as a function of amorphous carbon black	47
Fig 5.14	BET analysis of nanocarbon N220	50
Fig 5.15	BET analysis of nanocarbon N115	51
Fig 5.16	Apparent porosity as function of graphite	51
Fig 5.17	Bulk density as a function of graphite	53
Fig 5.18	Modulus of rupture as a function of graphite and nanocarbon black	54
Fig 5.19	Width loss caused by the slag as a function of graphite and nanocarbon	55
Fig 5,20	Slag corrosion resistance, comparing N115 and N220 for (a) 15% graphite content (b) 12% graphite content (c) 9% graphite content (d) 6% graphite content	56
Fig 5.21	Spalling resistance of zirconia graphite refractory as a function of graphite	57
Fig 5.22	Modulus of elasticity as a function of graphite content	58

Fig 5.23	SEM image of Zirconia-graphite refractory with (a) 15 wt% graphite with 0.5% nano carbon, (b) Slag metal interface 15wt% graphite with 0.5% nanocarbon (c) 12wt% graphite with 0.5% nano carbon (d) Slag metal interface for 12 wt% graphite with 0.5% nanocarbon (e) 9wt% graphite with 0.5% nano carbon (f) slag metal interface for 9wt% graphite with 0.5% nano carbon (g) 6wt% graphite with 0.5% nano carbon (h) Slag metal interface for 6 wt% graphite with 0.5% nanocarbon.	59
Fig 5.24	Oxidation resistance test as a function of graphite	61
Fig 5.25	Apparent porosity as a function of nanocarbon	63
Fig 5.26	Bulk density as a function of nanocarbon	63
Fig 5.27	Modulus of rupture as a function of nanocarbon	64
Fig 5.28	Width loss caused due to slag as a function of nanocarbon	65

LIST OF TABLES

Table 4.1	Chemical composition of CaO stabilized zirconia weight percent	17
Table 4.2	Chemical composition of silicon metal	18
Table 4.3	Chemical composition of Novalak resin	19
Table 4.4	Characteristics of nanocarbon black	20
Table 4.5	Chemical composition of nanocarbon black	20
Table 4.6	Batch composition of zirconia graphite refractory by wearing different grades of graphite	21
Table 4.7	Batch composition of zirconia graphite refractory by inclusion of amorphous carbon black	22
Table 4.8	Batch composition of zirconia graphite refractory by inclusion of nanocarbon black (N220) and decreased the % of graphite	22
Table 4.9	Batch composition of zirconia graphite refractory by inclusion of nanocarbon black (N115) and decreased the % of graphite	23
Table 4.10	Batch composition of zirconia graphite by increasing the % of N115 at 9wt% graphite and comparison with standard specimen	23
Table 4.11	Mixing sequence of various raw material	24
Table 4.12	Chemical composition of LD slag	32
Table 5.1	Batch formulation of zirconia graphite refractory with varying fixed carbon %	35
Table 5.2	Batch composition of zirconia graphite refractory by inclusion of amorphous carbon black	42
Table 5.3	Batch composition of zirconia graphite refractory by decreasing graphite % and inclusion of nanocarbon N220	49
Table 5.4	Batch composition of zirconia graphite refractory by decreasing graphite % and inclusion of nanocarbon N115	50
Table 5.5	Batch formulation of increase in % of nanocarbon on 9 wt% graphite in zirconia graphite refractory	62

ABSTRACT

Zirconia graphite refractory is generally used in slag like zone of sub entry nozzle in continuous casting. Zirconia graphite refractory has superior thermal shock resistance and corrosion resistance as compared to MgO-C and Al₂O₃-C refractory. The effect of graphite on zirconia graphite refractory is not well documented. Therefore, in the present work an attempt has been made to evaluate the effect of graphite on the properties of zirconia refractory. Graphite can be classified in terms of fixed carbon content. Therefore, in the present work three different types of graphite with varying fixed carbon content has been used. The fixed carbon content in the graphite was varied from 99%, 94% and 80%. The amount of zirconia was kept 82% and that of the graphite was 18%. Other processing parameter and other ingredient concentration were kept fixed throughout the work. Refractory samples were fabricated using cold isostatic method and it refractory samples were coked in 1000°C in reducing atmosphere. The effect of fixed carbon percentage on the apparent porosity, bulk density, spalling resistance, oxidation resistance has been evaluated. In the next stage some 2% of graphite has been replaced with amorphous carbon black. All processing parameters were kept same as before and the effect of amorphous carbon black on the properties of refractory has been examined. The next stage the amount of graphite has been reduced from 18% to 15%, 12%, 9% and 6%. With reducing graphite content 0.5% of nano carbon has been introduced in the matrix. Two types of nano carbon have been used. They have same DBPA number but differ in iodine absorption number. Processing parameters was kept constant as before. The effect of nano carbon on the properties of zirconia refractory has been examined. Apparent porosity, bulk densities have been measured and the effects of nano carbon on the on AP and BD values have been evaluated. The corrosion resistance was tested in rotary drum method. The operating temperature during corrosion resistance was 1550°C with two times replacement of slag and molten metal and carrion resistance has been measured in terms of width loss of the samples. The cold modulus of rupture was measured and the effect of nano carbon on CMOR values has been evaluated. The thermal spalling resistances have been performed by two different methods, first, by small prism method and second, water quenching method. The thermal spalling resistances have been carried out to observe whether samples can withstand more than 10 cycles. Modulus of rupture for all the samples has been calculated to evaluate thermal spalling resistance of the refractory. Oxidation resistance test has also been done in oxidizing atmosphere at 1200°C. After optimizing the amount of nano carbon content and graphite content, the percentage of nano carbon has been changed to 1% and 1.5%. The effect of nano carbon concentration on the physical, mechanical, thermal and corrosion resistance properties of zirconia refractory has been evaluated.

CHAPTER 1 INTRODUCTION

In recent year due to increase in the demand of large quantity of steel with uniform characteristic had attracted metallurgical industries towards continuous casting of steel. It is a mechanism by which steel has been continuously cast. In order to ensure smooth and stable casting operation special refractories material has been employed such as ladle shrouds (LS), slide gate plates (SN Plates), monoblock stopper(MBS), tundish nozzle and submerged entry nozzle(SEN).

Submerged entry nozzle play a vital role during the flow of molten steel from tundish to the mold. It is used to prevent the molten steel from being coming into the direct contact with the atmospheric oxygen and avoid the splashing during the flow of steel from tundish to the mold, so as to ensure a good quality of steel has been produced during the casting process. The life of Sub entry Nozzle depends upon its capability to withstand against the attack of molten slag. Therefore, slag line level of Subentry Nozzle is subjected to high risk of corrosion. The outer periphery of the slag line level of Sub Entry Nozzle is in contact with the reactive fused mold powder. These mold powder consist of CaF_2 which is having low basicity, and low viscosity, corrodes the refractory at the mold slag line level.

Generally oxide refractory couple with graphite material are used in the slag line level. At high temperature the graphite present in the refractory start oxidizing. thereby, allow direct exposure of oxide refractory to the molten slag. As a result molten slag attack the oxide refractory surface and cause loosening of bond between oxide and graphite. Consequently, refractory surface start corroding and can bring about a premature rupture of the slag line level and casting stoppage.

The improvement in the corrosion resistance of the refractory material used in slag line level helps in achieving longer sequence casting of steel. As aluminous or magnesian refractory could not cope with the corrosion by the mold powder that's why, zirconia-graphite material has been applied to the slag line level due to its excellent corrosion resistance over other refractory material.

The corrosion resistance of Zirconia-Graphite refractory increases with an increase in the zirconia content in the Zirconia-Graphite refractory. But, as the zirconia has low thermal conductivity, the high percentage of zirconia undergoes substantial thermal expansion. Thereby, increases the possibility of spalling crack in the slag band of Subentry nozzle. Whereas, increase in the graphite content improves thermal spalling resistance but this results in poor refractoriness. Researcher had done experiment to optimise the Zirconia and graphite composition. They found that Zirconia content of more than 80% will be prone to spalling crack for standard pre-heating practice of SEN. However, zirconia upto 85% can survive against spalling for a strict and controlled pre-heating practice of SEN.

As thermal shock resistance and corrosion resistance both are ambivalent properties, it is difficult to improve both simultaneously. To overcome this drawback nano materials have been incorporated in the structure. As nano material is having high specific surface area it easily disperse among space between coarse, medium and fines particle of the refractory raw materials. Thereby, fill up the voids of the aggregates. The addition of small amount of nano material gives remarkable improvement on the performance of the refractory.

As nano carbon black has an advantage over graphite that it is having high specific surface area and has having a degree of aggregates growth. Thereby, it has a potential to reduce the percentage of graphite without compromising the characteristics of graphite in present work it has been study the effect of various grades of graphite and can easily cover the zirconia present in the refractory thereby, helping in increasing the percentage of Zirconia, in the zirconia-graphite refractory.

The present studies aim to develop a zirconia-graphite refractory for Subentry nozzle. The studies has been carried out in three phases. In first phase the effect of varying the percentage of fixed carbon present in the graphite on zirconia-graphite refractory has been studies in order to achieve high thermal shock resistance as well as high corrosion resistance in zirconia-graphite refractory. In second phase with an aim to increase the zirconia percentage upto 90% with high corrosion and spalling resistance has been studies. In this phase with a use of optimise fixed carbon graphite, the graphite percentage has been reduced and inclusion of nano carbon black into the zirconia graphite refractory has been done. So that high thermal spalling resistance along with high corrosion resistance can be achieved. In third stage, an attempt has been made to optimise nano carbon percentage with fixed graphite percentage on zirconia-graphite refractories has been studies. Each step had been characterized.

CHAPTER 2 LITERATURE REVIEW

2.1 Continuous casting

Continuous casting is also known as “strand casting”, is the process in which molten steel is being solidified into a "semifinished" billet, bloom, or slab by subsequent rolling in the finishing mills. the process of metal casting through the mold has been depict in Fig.2.1 . The casting takes the two dimensional profile of the mold but its length is indeterminate. The high melting point and reactive nature of steel at high temperatures had made steel a difficult material to cast. Therefore, in continuous casting of steel, special refractories are being employed to control the flow of the steel and protect the steel from oxidation during as it poured from steel ladle to tundish and from tundish to the casting mold. Refractories products used in Continuous casting are Slide gate plates, Monoblock stopper, Ladle shrouds and Submerged entry nozzle. Among these, Slide gate plate and Monoblock stopper is used to control the flow of molten steel below tundish whereas Ladle shrouds and Submerged entry nozzles (SEN) are employed to protect the molten steel from oxidation during the steel transfer and casting operations [1]

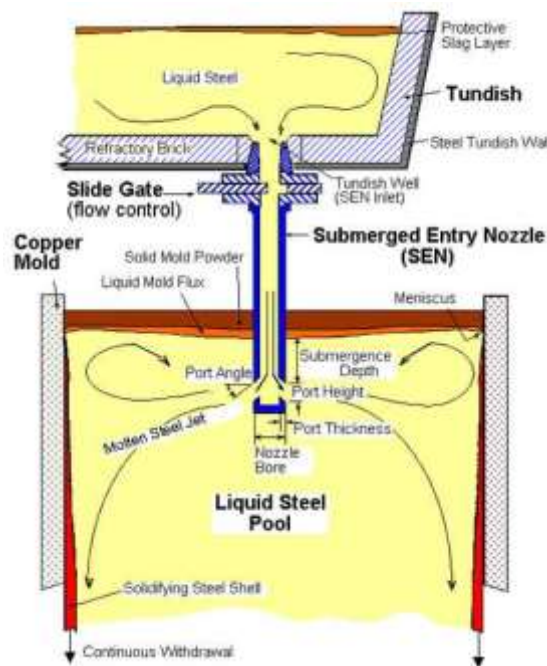


Fig1: Schematic diagram of submerged Entry Nozzle

2.2 Necessity of Subentry Nozzle

In order to ensure a good quality of steel which is free from all type of defects such as unwanted porosity, crack etc. mold is either vertically oscillated or a lubricant is added with the molten steel in the mold for smooth passage. These lubricants contain CaF_2 which prevent the molten steel from being sticking to the walls of the mold. It also helps the slag, which may get entrapped in the molten steel if not removed during casting, to come out at the top of the pool to form a floating layer at the surface of the molten steel. In this way, the floating slag can also prevent the steel from being oxidized. Therefore, in order to ensure the smooth passage of molten steel below the surface of the slag layer, so that molten slag can be retained on top surface of the molten steel, a nozzle is used known as submerged entry nozzle or Subentry nozzle (SEN).

2.3 Submerged entry nozzle

Submerged entry nozzle plays a vital role in ensuring smooth and stable casting operation. It is used to connect the tundish and the mold in the continuous casting of steel and prevent the molten steel from being oxidized. It comprises of a nozzle body having a central bore extending axially from an inlet end to an outlet end. The nozzle body is preferably made of an alumina-Graphite refractory material and the slag line sleeve section of SEN is made up of carbon bonded zirconia-graphite refractory material as shown in Fig 2. The body and sleeve are compressed together and then fired. The sleeve is located in the region where the SEN is in contact with the slag/metal interface.

2.4 Function of Subentry nozzle

- (i) **Prevention of molten steel from being oxidized:** In order to improve the quality of the steel and prevent it from internal defects. SEN is employed to avoid direct contact of molten steel with the atmospheric oxygen during the flow of steel from tundish to the mold.
- (ii) **Avoidance of molten steel from splashing:** In order to ensure laminar flow of molten steel SEN is employed so that splashing of molten steel during the flow from tundish to mold can be avoided. The bottom portion of SEN is immersed in

the molten steel present in the mold. Thereby, SEN prevent the dissolution of slag in the molten steel and improve in the quality of steel.

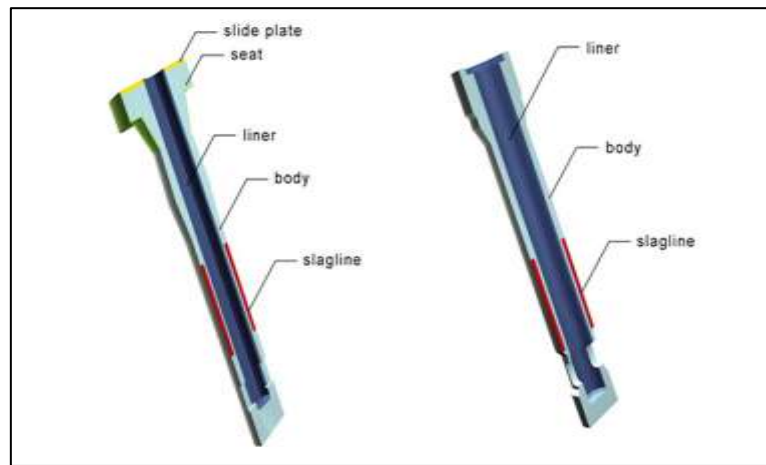


Fig 2.2. Different parts of Sub entry nozzle

It mainly consists of following part as shown if Fig 2.2:

- Body part
- Inner liner
- Seat area
- Port Area
- Slag band area

2.5 Body part

The dissolved oxygen present in the steel during casting operation results in deterioration of the quality of steel by creating unwanted porosity, crack and other internal defects. Therefore, in order to prevent the molten steel from being oxidize Aluminium metal, ferromanganese, or ferrosilicon are commonly added as a de-oxidizer. This aluminium react with dissolved oxygen or iron oxide present in the molten steel to form finely-dispersed aluminium oxide, some of which floats with the slag above the molten steel and some of which remains as highly-dispersed micro particles in the solidified steel. During Continuous Casting, these extremely fine dispersed particles of Al_2O_3 had a tendency to react and stick to the refractory surface in contact with steel. Thereby, blocking the inner bore of the SEN and obstruct the smooth passage of molten steel. This phenomenon of obstructing the flow of molten steel by gradual build-up of Alumina is known as *Alumina clogging*. This gradual

buildup of alumina causes problems in the flow of molten steel and may eventually cause blockage in the Subentry Nozzle. Therefore, body part of SEN is generally made up of Alumina-graphite material. As Alumina present in the graphite start eroding along with the molten steel. Thereby, it does not allow the Alumina present in the steel to adhere to its refractory surface. Consequently, alumina clogging had been prevented.

(a) Inner liner

In order to ensure smooth and stable flow and prevent the refractory material from Alumina clogging the Subentry nozzle inner bore is lined with high temperature glaze coating. These glaze material form glassy coating at the time of preheating the nozzle. Thereby, prevent the carbon of from being oxidized which in turn help in reducing the direct contact of molten steel with oxide refractory material and prevent the adherence of alumina material to stick to the inner wall of Subentry nozzle. Therefore, preheating of SEN may be useful to achieve this purpose. B Prasad et al[2] had tried to optimize the preheating schedule. They reported lower preheating temperature leads to crack formation in SEN due to thermal spalling, whereas over preheating leads to glaze evaporation/ carbon oxidation and contribute to low life of SEN due to higher erosion. They found an Optimum preheating temperature is about 950-1050⁰C for a duration of 90 to 150 mins. Y. M. Lee et al[3] also define the importance of proper preheating schedule so that the glassy oxide form coating over the Zirconia-Graphite and prevent the carbon from being oxidise thereby, increasing the life of SEN. A Sasaki et.al[4] had tried to prevent the cracking of inner bore material, made up of MgO-C by applying an intermediate layer called stress buffer layer of 0.5mm thickness between the main part and the inner bore part. This type of structure is called triple-layered structure nozzle. The intermediate layer is composed of 77wt% carbon and 23wt% Al₂O₃. Al₂O₃ is added to this layer in order to increase its refractoriness resulting in highly porous structure with apparent porosity of 71%, and the elastic modulus at high temperature region (~1400°C) is 5×10⁻³ GPa [4]. The Finite Element Method analysis showed that the triple-layered structure nozzle with applied intermediate layer is able to fully absorb the stress generated by the expansion of the inner bore material in contrast to the SEN which consist of the two-layered structure[4].

(b) Seat area:

Seat areas of subentry nozzle are subjected to high wear due to the relative motion between the monoblock stopper and subentry nozzle. It is also subjected to high erosion due to the turbulence created by the molten steel at the time of entering the SEN. Therefore, refractory material used in seat area of SEN should have high wear and erosion resistance. Therefore, magnesia-graphite is used in seat area in order to ensure superior erosion resistance against molten steel flow at the stopper inlet.

(c) Port Area:

The direct flow of molten steel in vertical downward direction is avoided as it may create turbulence in the molten steel present in the mold. This turbulence may cause aluminium compound remain in dissolve position in molten steel which in turn deteriorate the properties of steel. Therefore, The base of SEN had been closed and allowed the molten steel to diverge in two different directions, for this purpose two ports are provided at the bottom portion of the SEN. As the bottom portion is subjected to high risk of alumina clogging therefore, port area is made up of alumina-graphite material.

2.6 Slag Band of SEN:

The sleeve of Slag band as described above are subjected to high risk against molten slag as it may corrode the sleeve area. Therefore, refractory material used in slag band of subentry nozzle must have following properties:

- High Spalling Resistance
- Corrosion resistance against molten steel slag
- High Oxidation Resistance

(a) High Spalling Resistance:

As Subentry nozzle is subjected to high thermal shock at the time gap between preheating the nozzle and first consignment of molten steel flowing through the nozzle. Within this small time gap nozzle is suffered from high temperature gradient. Therefore, nozzle refractory material should be such that it should have high thermal conductivity. As high thermal conductivity refractory material will help in passing the heat from inner wall to outer wall as shown in Fig 5.3. Thereby producing less temperature gradient due to Fourier

law of heat transfer. As temperature gradient is less, there, it helps in relieving the stress concentration at the refractory body which in turn help in avoidance of the crack propagation.

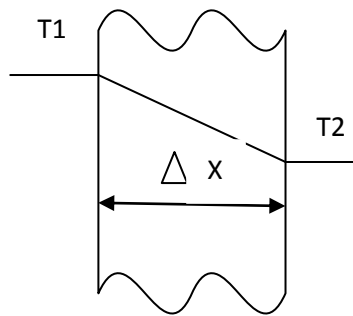


Fig 5.3 depicts Heat transfer from hot surface to cool surface

(b) Resistance against molten steel Slag:

In order to facilitate the smooth passage of the partially solidified casting through the mold, it is necessary to provide lubrication between the metal being cast and the copper mold walls. For this purpose flux type materials (generally consist of fly ash, blast furnace slag and high melting point silicates) is used as a lubricants which on melting gives a glass-like lubricant. In order to control the viscosity and fusion temperature of the lubricant, CaF_2 is added but this CaF_2 presence will cause the erosion of the refractory material presence in the sleeve area of slag band, thus contributing to the failure and ultimate breakage of the SEN at the slag line in the mold[5]. Therefore, the outer wall of SEN at the slag band should be made up of such an oxide refractory material that can prevent the inclusion of CaF_2 .

(c) High Oxidation Resistance:

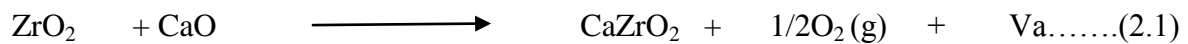
The carbon present in the refractory had a tendency to oxidise at a temperature greater than 600°C . There by, causing the loosening of bond between oxide refractory and carbon which in turn help in slag penetration inside the refractory material. Therefore, the refractory material should be used with suitable antioxidant.

(d) Technique to solve the above problem: In order to overcome above difficulties researcher had tried various refractories materials and optimizes the existing refractory material for slag band of SEN. So, that the refractory material can withstand against molten slag . For this purpose they had adopted different Technique which are given below:

- Use of different oxides material.
- Optimization of Graphite percentage
- Addition of Antioxidant
- Addition of Binder
- Addition of Nano Material

(e) Uses of different oxide material:

B. J. Monaghan et al [6] had investigated the dissolution behaviour of alumina, spinel and zirconia against steel containing $\text{CaO-SiO}_2\text{-Al}_2\text{O}_3$ as a slag . They had done experiment and found that the rate of dissolution of alumina refractory in $\text{CaO-SiO}_2\text{-Al}_2\text{O}_3$ slag is slower than that of spinel. This is principally because amount of Al_2O_3 present in Al_2O_3 refractory is more in comparison to spinel. Whereas, zirconia on reacting with CaO present in the slag produces a gas bubble (Equation 2.1), this bubble formation act as a barrier for Zirconia dissolution in slag.[6]



where Va represents a vacancy within the CaZrO_2 structure.

LI HONGXIA et al [7] had studied the effect of fused ZrO_2 raw material with different microstructure on corrosion resistance. The three different fused ZrO_2 raw materials are (1) fused CaO partial stabilized ZrO_2 raw material used in conventional Sub entry nozzle, (2) Dense CaO partial stabilized ZrO_2 raw material, (3) Y_2O_3 partial stabilized ZrO_2 raw material. The mold powder used to test these raw materials contains (Al_2O_3 , SiO_2 , CaO , F, carbon, Na_2O). They found that dense CaO partial stabilized ZrO_2 and Y_2O_3 partial stabilized ZrO_2 raw material along with graphite showed better corrosion resistance. As the density of stabilizer increases less will be the grain boundary and the chances of liquid penetration decreases as a result corrosion resistance improved. [19].

T Imaoka et al [8] had found that the mold powder are normally very corrosive toward Alumina-Graphite refractories and have necessitated the development of Zirconia-Graphite sleeves on the Submerged Entering nozzle used in the Slagline. The use of Zirconia-Graphite Sleeves has increased the normal life expectancy of the average Subentry nozzle up to 2-6 ladles of steel during Continuous Casting. S J lee et al[9] had tried Zirconia mullite, High Purity Zirconia-Graphite and Sintered Zirconia as a sleeve in slag band of Subentry nozzle. They found that addition of ZrO_2 in mullite composition proved advantageous on high residual Oxygen free cutting grades of steel, and addition of High purity Zirconia-Graphite with minimal fluxing agent provide high resistance to corrosion compared to conventional Zirconia-Graphite composition. Whereas, sintered ZrO_2 sleeves should be fired precisely to control the pores size and matrix microstructure required to improve thermal shock resistance and corrosion resistance.

Optimization of Graphite percentage:

A Sen et al[10] had tried to optimise the ratio of zirconia and graphite in the composite. They took the four compositions of zirconia and graphite by varying the percentage of Zirconia from 75% to 90% in an interval of 5% and an antioxidant (1%) and CaO (4%) and carried out rotary drum test and spalling test and found that composition with 85% zirconia and 10 % graphite gave the optimum composition with higher corrosion resistance and higher spalling resistance. D Yoshitsugu et al[11] had studied the relationship between Apparent porosity and Corrosion resistance and effect of variation in graphite percentage (3-21%) on durability of Zirconia-Graphite. They found that for same Zirconia-Graphite composition decrease in Apparent Porosity causes increase in corrosion resistance but as the Zirconia content increases, graphite content decreases leads to an increase of apparent porosity because of poor compatibility of the Zirconia-Graphite mix, resulting in poor corrosion resistance of ZG mixture.

(f) Role of Antioxidant:

R. parodi et. al [12] had studied the effect of different metallic powder (Al, Si, Mg, Ca) in carbon contain refractories. MgO-C or Al₂O₃-C brick were taken as test Brick. They had prepared 5 batch of MgO-C with different antioxidant (No antioxidant, Al, Al-Si, Mg-Al, Si-Mg-Al) with 10% fixed carbon and found that composition with Mg-Al, Si-Mg-Al show remarkable difficulties in mixing and molding (due to probable interaction with Resin) whereas composition with Al antioxidant shows -51% oxidation resistance and Al-Si shows -67% oxidation resistance but Al shows problem of Hydration during coking at 1000⁰C so Al-Si (87.4%Al & 12.6%Si because of eutectic point) had been the best antioxidant which give higher global properties than composition with Al as an antioxidant.

They had also prepared 3 batch with 76% Al₂O₃ and 10% Fixed carbon with 3 different antioxidant 3% of Si, Al, Al-Si and found that oxidation resistance of Silicon composition is -35.5%, Al composition is -14.2% and Al-Si composition is -18.4% because of oxygen affinity towards aluminum is higher than silicon but this result in decrease in MOR whereas carbon bonded Si convert into SiC between 1000-1200⁰C and unbounded convert to cristoballite, as temperature rise in between 1200-1500⁰C. Cristoballite react with corundum to form a mullitic matrix but HMOR is comparable to Al composition so Al-Si additive to be the best compromise between oxidation strength and thermo-mechanical strength.

A Sen et al [10] had studied the effect of antioxidant on the zirconia-graphite composite. they had varied the percentage of antioxidant by 1.2wt%, 3.2wt% and 5.2wt% and found that 3.2 wt% of antioxidant show better corrosion resistance and higher spalling resistance by melting itself and forming a glassy coating on the carbon particles and thus protect them from oxidation during preheating of SEN. B Prasad et.al[2] had studied the effect of inclusion of B₄C in zirconia-graphite composite. They conducted the experiment with varying the percent of B₄C by 0.0%, 0.5%, 1.0%, and 1.5% and found that there is no substantial improvement in room temperature properties like AP,BD and MOR but in oxidation & corrosion test the samples with 1.0 % B₄C had shown substantial improvement as compare to the base composition Actually during heat treatment the B₄C forms B₂O₃ & generates glassy phase, which acts as oxidation resistance to the mix. However further increase in B₄C % (S4) had not shown much improvement.

LI HONGXIA et al [7] had studied the effect of different antioxidant on the Zirconia-Graphite composite. They had chosen Aluminium powder, Boron carbide and Boron nitride as an anti-oxidation and found that Boron Nitride showed corrosion resistance of 0.99 mm/hr which is far better than other antioxidant.

(g) Role of Resin Binder:

Shin-ichi Tamura et al [13], had concentrated on the improvement of corrosion resistance and spalling resistance of MgO-C brick by modifying pore structure and controlling bond strength. They had used three kinds of Binder such as Hybrid Binder (HB) and High performance Hybrid Binder (HHB). In Hybrid Binder appropriate amount of carbon Black is suspended and in HHB Binder Compound graphitized black with B₄C was added. They used 3.2% of these binders in combination with 1.5 % Aggregates types of Nano Carbon black and found that oxidation resistance improved remarkably of MgO-C refractory containing HHB.

A. Gardziella et al [14] had conducted an orientative test on impregnation of Resin Binder in bauxite bricks to determine which type of Resin exhibits a specific range of properties. They had selected five compositions of phenolic resin (A,B,C,D,E) among them A,B,C are Self-curing aqueous Resoles of different viscosities and condensation level, Resole D is a catalytically accelerated resole and E is a Novalak Solution containing hexamethylene tetramine as a curing agent. They found that there is a 10-12% drop in Porosity after impregnation. The cold crushing Strength of Resoles A,B,C is approximately twice then Resoles D and thrice as compared to Novalak Solution E. Again these Resins are used to impregnate Carbonized Bauxite Bricks and found that Lowest open Porosity coupled with the highest bulk Density is achieved and CCS is achieved in relatively low molecular mass, self-curing resole B. Slag Resistance test showed that Resole B and Novalak solution showed lowest attrition level but the problem associated with the resoles is that they possess only limited storage life at ambient temperature and should be stored at 5-10°C for this reason their main effort to develop Resin E. D Yoshitsugu et al [11] had correlated the apparent porosity with corrosion resistance and developed unique resin to densify the Zirconia-Graphite mixture. They had added Unique resin to a Zirconia-Graphite mixture in which ZrO₂ content is greater than 86% and found that unique resin produces a microstructure of carbon fiber through firing which results in less thermal expansion, excellent mechanical strength and low elasticity. Both of the thermal spalling resistance and the corrosion resistance are improved due to the denser structure. Yong-ho Cho et al [15] had evaluated the properties of porous

partially stabilized zirconia (PSZ) ceramic containing phenolic Resin as a binder at various Relative humidity(RHs). They exposed the mixture of CaO-PSZ and 5wt% binder at different RHs 25,50,75,and 95%for 1hr before compaction and found that the young modulus, green density and sintered density decreases and porosity increases gradually till 75% RH and beyond that decreases rapidly. At 25% RH the specimen exhibited a uniform and dense microstructure, whereas at 95% RH the microstructure of the specimen formed agglomerates, this is because the moisture in the humid atmosphere act as a catalyst for the decomposition of hexamine as a curing agent as a result enhanced the curing rate and the degree of curing. Deterioration of mechanical properties was also observed during curing of the phenolic resin during fabrication of porous PSZ ceramic under high temperatures and high humidities.

2.7 Role of Nano Material in the Development of refractories

- Role of Nano Zirconia
- Role of Nano Carbon

(A) Role of Nano Zirconia:

A Sen et al[10] had tried to incorporate nano zirconia in a variation of 0%, 1%, 2% in conventional Zirconia-Graphite composition (85wt% Zirconia and 15wt% graphite) and found that 1% nano zirconia addition will improves both corrosion resistance and spalling resistance of Zirconia-Graphite composite by forming coating over the surface of Graphite preventing its oxidation and there by improve corrosion resistance of zirconia-Graphite composite. J .K. Sahu et al [16], had focused on the improvement of erosion resistance of Mono block stopper (MBS) by incorporation nano non-oxide antioxidant to Al_2O_3 -graphite composite to achieve higher life of MBS. Nano non-oxide antioxidant of 5wt% formed a protective layer on the surface of carbon. This protective layer improves the oxidation resistance by absorbing the available oxygen and reduces oxygen availability for carbon. Therefore, it does not allow oxygen to penetrate it and oxidize carbon there by increasing the life of MBS. A Sen et al [10] had tried to vary the percentage of Nano–zirconia by 0.8%, 1.2%and1.6% keeping the antioxidant percent to 3.2% and found that Apparent Porosity decreases and Modulus of Rupture increases with increasing amount of nano zirconia.

(B) Role of Nano Carbon:

R.P.Rana et al [17] had tried to investigate the effect of nano carbon on MgO-C brick. They had varied the Nano-Carbon percentage from 0.3%, 0.6%, 0.9% by keeping the graphite percentage constant to 3wt% and compared their results with conventional 10wt% graphite in MgO-C brick and found that MgO-C brick containing 3wt% graphite and 0.9wt% Nano-Carbon had better thermo-mechanical properties than conventional 10wt% graphite. This may be due to the Nano Carbon having a graphitic nature. Thereby, Nano Carbon does not allow the slag to penetrate through the refractory material and hence improves the corrosion resistance of the MgO-C brick. Nano Carbon also had high thermal conductivity. Thereby, improves spalling resistance. Also, Nano carbon had high specific surface area it may fill up the voids between the aggregates. Thereby, improve oxidation resistance of the MgO-C brick. Y Matsuo et al [18] had tried to increase the percentage of addition of Carbon Nano Fibre (CNF) up to 0.4% in conventional MgO-C bricks (85wt% MgO and 15wt% Graphite) and found that Bulk Density increases with the increase in CNF percentage. They had also investigated the combination of CNF with addition of metal and pitch and found that Apparent Porosity of MgO-C brick incorporating the CNF with metal are remarkably lowered and Bulk Density is increased significantly, whereas effect of pitch is not favourable for the densification of the material, the mechanical strength increased by approximately 5.5 times. This is due to absorption of the crack by CNF network surrounding MgO grain. Therefore CNF addition will cause the strengthening of the MgO-C brick.

Y Shiratani et al [19], had studied the effect of nano carbon on the MgO-C SN plates and tried to improve the strength and spalling resistance of MgO-C SN plate. They used Carbon Nano Particles, Hybrid Graphite Black (HGB) and Hybrid High performance Binder (HHB) as a raw material. They prepared three samples in first they incorporate only Carbon nano particles of single sphere type with Hybrid Binder which can improve only strength but not spalling resistance. In Second they incorporate Carbon nano particles of aggregate type with Hybrid Binder which can improve only spalling resistance but not strength and in third they incorporate both Aggregate type nano Carbon black and Hybrid graphite black with high performance hybrid Binder by suspension method, and found that third showed higher Young modulus, higher thermal resistance and an excellent oxidation resistance.

Shin-ichi-Tamura et al [20] had used different combination of single sphere type nano carbon Black and Aggregate type nano carbon black. They used these types of Carbon Black to improve the corrosion resistance and thermal shock Resistance of the MgO-C brick and found that as an amount of addition of aggregate type nano carbon black increases the elastic

modulus decreases as a result thermal shock resistance improved and only 1.5% Nano carbon Black give the same spalling resistance as 18% flake graphite H Hattanda et al[21] had studied the effect of nano carbon and Hybridized Graphite black (HGB) on the Alumina-Graphite SN plates and tried to improves the strength and spalling resistance of Alumina-Graphite SN plate. They had observed by increasing the percentage of nano carbon Black to 1% will improve the Spalling Resistance and by inclusion of 1% HGB will improves the oxidation Resistance but further increase in nano carbon and HGB will detoriate the properties. Furthermore, they had showed the application of nano structured matrix to Carbon brick for blast furnace Carbon brick are used in bottom area of blast furnace therefore required to resistance against erosion. They had tried HGB with TiC for carbon brick and nano Carbon black. They had fixed the percentage of nano carbon fixed to 2 %. By increasing the percentage of HGB to 2% will increase the oxidation resistance to twice the conventional ones.

It can be concluded from the literature review that the recent trend in graphite based refractory are leading towards the minimization of graphite content in refractory. Significant amounts of work were also observed towards replacement of graphite with other form of carbon like amorphous carbon black, nano carbon etc. The effect of nano carbon on the graphite based refractory has been reported for MgO-C and Al₂O₃-C refractories. It has been reported that nano carbon has significantly increased thermo-mechanical as well as corrosion resistance properties of graphite based refractory. In case of ZrO₂- graphite based refractory, availability of documents are not plenty. The mechanism of graphite on ZrO₂ based refractory is also not well understood. Some indirect evidences can be concluded on the basis of MgO-C and Al₂O₃-C refractory. The effect of purity of graphite and its effect on thermo-mechanical properties of ZrO₂ based refractory also not been reported. There was also no literature available on effect of nano carbon on the mechanical, physical and corrosion properties of Zirconia-graphite refractories. Most of the commercially available Zirconia-graphite refractory generally has 80-85% zirconia and not much literature was available beyond greater than 85% zirconia content refractory. In the present work, this is the first attempt in the field of zirconia graphite refractory, to reduce the percentage of graphite hence increasing percentage of zirconia, has been taken. The effect of purity of graphite on the properties of refractory will also be evaluated in the present work. For the first time, the effect of nano carbon with decreasing percentage of graphite in refractory will also be evaluated.

CHAPTER 3 OBJECTIVE

The slag line level of subentry nozzle has been prone to high risk of corrosion and spalling crack produced by the molten slag. Therefore, Zirconia has been used in the outer periphery of the slag line level due to its high corrosion resistance properties against molten slag. Graphite is added to zirconia in order to achieve excellent thermal shock resistance. so that refractory used in slag line level can achieved high thermal spalling resistance and high corrosion resistance. As increased amount of graphite reduces the refractoriness of the zirconia-graphite refractory is also a major concern for steel industries as well for the environment. To overcome this drawback nano carbon has comes into play. With inclusion of small amount of nano carbon black to the zirconia graphite refractory the percentage of graphite has been greatly reduced.

Objective of the present studies has been given below

1. Development of zirconia-graphite refractory and effect of variation in the fixed carbon percentage of graphite on zirconia- graphite refractory.
2. Effect of replacement of some amount of graphite by amorphous carbon black in zirconia-graphite refractory.
3. Effect of reducing the graphite percentage by inclusion of nano carbon black into the zirconia-graphite refractory.
4. Effect of increasing the percentage of nano carbon black into a fixed percentage of zirconia-graphite refractory.

CHAPTER 4 EXPERIMENT WORK

4.1 Raw materials

(a) Calcia stabilized Zirconia

Calcia stabilized zirconia is a form of partially stabilized zirconia. The partially stabilised zirconia is produced by an electro-fusion of zirconia in combination with controlled quantities of calcia. Calcia is preferred over other oxides due to the stability of cubic phase at all temperatures, whereas the magnesia- or yttria- stabilized zirconia reverts to the monoclinic structure at low temperatures, so calcia stabilized ZrO_2 is preferred.

Properties of CaO stabilized zirconia:

- Excellent thermal shock resistance
- Uniform co-efficient of thermal expansion,
- High abrasion resistance at high temperature
- High corrosion resistance at high temperatures.

In the present work CaO stabilized ZrO_2 of different mesh size, termed as coarse, medium and fine were taken as a raw material. This mesh size has been followed throughout the work. The chemical composition and Particle size distribution are shown in Table 4.1 and Table 4.2 respectively.

Table 4.1 Chemical composition of CaO stabilized zirconia weight percentage

Chemical Composition						
Raw Material-----						
ZrO_2	CaO	SiO_2	Al_2O_3	MgO	Fe_2O_3	TiO_2
Zirconia(wt%) $\geq 94\%$	3.3-4.2	≤ 0.4	≤ 0.4	≤ 0.1	≤ 0.15	≤ 0.3

(b) Graphite

The graphite structure consist of hexagonal layer, in which the bonding is covalent and strong ($\sim 525\text{KJ/mol}$). These layers, which are called the basal planes, are stacked in an ABAB sequence. The inter layer are stacked together by vander waals bond which are weak bond ($< 10\text{KJ/mol}$). Graphite sublimes at 3700°C but start to oxidise in air at around 500°C . In present work graphite with different fixed carbon viz 99%FC, 94%FC and 80%FC were taken for studies.

Properties of graphite are as follow

- Low wettability from the melted products
- High cross-binding strength of the lamellae which ensure maintaining of high mechanical properties of the molded brick
- Low expansion coefficient
- Higher fracture energy
- Low young modulus
- High thermal conductivity which, together with the two preceeding item, ensures high thermal shock strength to the brick.
- Critical Spalling Rates for Various

(c) Silicon Metal

Silicon metal is used as an antioxidant, in order to prevent the carbon from being oxidise at high temperature. The percentage of silicon metal has been fixed to 0.5wt% throughout the work.

Table 4.3 Chemical Composition of Silicon Metal

Raw Material	Chemical composition		
	Si	Al_2O_3	Fe_2O_3
-----	97%	0.1%	0.7%

(d) Resin Binder

Phenolic resins are produced by reacting phenol and formaldehyde. Phenolic resins are of two type viz *resoles* or one-stage resins contain the necessary constituents (including catalyst) to be cured by heating without the need of any additional curing agent. *Novalacs* (two stage resin) require the addition of a catalytic agent prior to fabrication. The undesirable feature of phenolic resin is that volatile by-products are evolved during curing, hence high pressures are often necessary in composite production. In novalaks, molar ratio of phenol and formaldehyde is maintained at 1:0.2-0.8. novalak is thermoplastic and do not set in presence of heat. It hardens to thermoset polymer by addition of formaldehyde or hexamethyl tetra amine at temperature above 100⁰C. Resin binder of novalak types were used both as a powder form and at liquid state. In present work 6% of resin powder form and 6% of resin at liquid form were used.

Phenolic Resin had following excellent features:

- Its chemical affinity towards graphite and refractories aggregates make it easy to disperse.
- It is adhesive, which increases its base strength.
- It is thermosetting and has a high dry strength, which means that there is no significant expansion of the dried compact.
- It has a high content of fixed carbon that contributes to strong carbon bonding
- It is environmentally less harmful than tar pitch. [47]

Table 4.4 Chemical composition of Novalak resin

Properties	Liquid Resin
Non volatile Content (1 gm at 140 ⁰ C for 30 min)	76.4
Viscosity at 25 ⁰ C(cps)	715
Specific Gravity	1.22
pH	6.7
%FC	57.1
Volatile Content	2.3
Hexamine content	10.2

(e) Nano Carbon Black

Nano carbon black is a mixture of partially burned hydrocarbons. Nano Carbon black is produced by incomplete combustion of natural gas. Nano Carbon black occurs in the form of spherical particles with an average size ranging from 100 to 3,500 angstroms (Å). The particles are made up of layers of carbon atoms similar to the layers in graphite. The layers themselves consist of hexagons with carbon atoms situated at the vertices and separated from adjacent atoms by a distance of 1.42 Å. Unlike graphite, however, the layers in carbon black are curved rather than flat, which accounts for the spherical surfaces of the particles.

Table 4.5 Characteristics of Nano carbon Black

Raw material	Iodine Absorption No (gm/kg of Carbon)	DBPA (cm ³ /kg)	Nitrogen Absorption, specific SA (10 ⁵ m ² /kg)
N115	160	115	129-145
N220	121	115	112-126

Table 4.6 Chemical Composition of Nano Carbon Black

Raw Material	Volatile Content%	Ash%	Surface Area(m ² /gm)
N115	≤3%	-	143.23
N220	≤2.5%	≤0.5%	131.05

4.2 Fabrication of Zirconia-Graphite Refractory:

(a) Batch preparation:

Commercially available CaO stabilized zirconia of different mesh size, Coarser, Medium and Fines were taken, different size fraction has been taken in order to maintain the granulometry of the mixture. Natural flakes graphite of different fixed carbon percentage (99%, 94%, 80%), silicon metal powder, amorphous carbon black, nano carbon black, resin powder and liquid resin of novalak types were used as a starting raw materials for the fabrication of Zirconia-Graphite refractory.

Different Grade of Graphite (99%, 94%, 80%) with fixed Composition of ZrO₂-Graphite (72wt% zirconia and 18% Graphite) were fabricated first, and after finding an optimum grade

of graphite. In the first stage 2wt% of two different grades of graphite has been replaced by Amorphous Carbon Black in zirconia-graphite refractory, so that the total carbon percentages in the refractory remain constant. After finding the optimum graphite concentration composition from above studies, inclusion of 0.5wt% of two different type of nano carbon on zirconia-graphite refractory has been done by decreasing the Graphite percentage from 18 to 6 in a gap of 3%. After finding an optimum composition of ZrO_2 -Graphite refractories, finally some study has been on varying the percentage of Nano carbon from 0.5 to 1.5%. All the different batch compositions of ZrO_2 -Graphite refractory done in the present study are given in the following tables 4.7, 4.8, 4.9 4.10 and 4.11.

Table 4.7 Batch composition of Zirconia-graphite refractory by varying different grades of graphite.

Raw Material (wt%)		T-1	T-2	T-3
CaO stabilized ZrO_2	Coarser	23.8	23.8	23.8
	Medium	32.7	32.7	32.7
	Fines	25.5	25.5	25.5
Graphite	99%FC	18	-	-
	94% FC	-	18	-
	80%FC	-	-	18
Resin liquid		6	6	6
Resin Powder		6	6	6
Silicon Metal		0.5	0.5	0.5

Table 4.8 Batch composition of Zirconia-graphite refractory by inclusion of Amorphous carbon Black.

Raw Material(wt%)		T-4	T-5
CaO stabilized ZrO ₂	Coarser	23.8	23.8
	Medium	32.7	32.7
	Fines	25.5	25.5
Graphite	99% FC	16	-
	94% FC	-	16
Amorphous carbon Black		2	2
Resin powder		6	6
Resin liquid		6	6
Antioxidants		0.5	0.5

Table 4.9. Batch compositions of zirconia-graphite refractory by inclusion of Nano carbon black (N220) and decreasing the percentage of graphite.

Raw material (wt%)		T-6	T-7	T-8	T-9	T-10
Chemical composition	CaO-ZrO ₂	82	85	88	91	94
	Graphite(99%FC)	18	15	12	9	6
	Silicon	0.5	0.5	0.5	0.5	0.5
	Binder	12	12	12	12	12
	N220	0.5	0.5	0.5	0.5	0.5
Grain Size Distribution of ZrO ₂	Coarser	23.8	24.7	25.6	26.6	27.4
	Medium	32.7	34.1	35.3	36.4	37.7
	Fines	25.5	26.2	27.1	28	28.9

Table 4.10. Batch compositions of zirconia-graphite refractory by inclusion of Nano carbon black (N115) and decreasing the percentage of graphite.

Raw material (wt%)		T-11	T-12	T-13	T-14	T-15
Chemical composition	CaO-ZrO ₂	82	85	88	91	94
	Graphite(99%FC)	18	15	12	9	6
	Silicon	0.5	0.5	0.5	0.5	0.5
	Binder	12	12	12	12	12
	N115	0.5	0.5	0.5	0.5	0.5
Grain Size Distribution of ZrO ₂	Coarser	23.8	24.7	25.6	26.6	27.4
	Medium	32.7	34.1	35.3	36.4	37.7
	Fines	25.5	26.2	27.1	28	28.9

Table 4.11 Batch compositions of Zirconia Graphite by increasing the percentage of N115 at 9wt% Graphite and comparison with Standard specimen

Raw Material (wt%)		T-C	T-16	T-17	T-18
Chemical composition	CaO-ZrO ₂	82	91	91	91
	Graphite(99%FC)	18	9	9	9
	Silicon	0.5	0.5	0.5	0.5
	Binder	12	12	12	12
	N115	0.0	0.5	1.0	1.5
Grain Size Distribution of ZrO ₂	Coarser	23.8	26.6	26.6	26.6
	Medium	32.7	36.4	36.4	36.4
	Fines	25.5	28	28	28

(b) Mixing:

Mixers are used to homogenize and uniformly mix the solid compounds with the binding agent. In this process, the solids are placed into the mixer and homogeneous Heating & mixing is done in Sigma mixer which is having a gross volume 75 lits, horse Power 570.5, Gross weight 510N whose two S-shaped roller is rotating at 18-27 rpm. The temperature of the Heater is 180⁰C whereas the temperature of the mixture is about 75⁰C.

Table 4.12. Show the mixing sequence of various raw materials.

Steps	Mixing Sequence	Mixing time(min)
1	ZrO ₂ +graphite+Antioxidants	5
2	Addition of Powder Resin	5
3	Addition of Liquid Resin	10
4	Mixing	30
5	Unloading	

Steps	Mixing Sequence	Mixing time(min)
1	ZrO ₂ +graphite+Antioxidants+ Nano Carbon	5
2	Addition of Powder Resin	5
3	Liquid Resin	10
4	Mixing	30
5	Unloading	

Steps	Mixing Sequence	Mixing Time(min)
1	ZrO ₂ +graphite+Antioxidants	5
2	Addition of Powder Resin	5
3	Liquid Resin+MEG+ Nano Carbon	10
4	Mixing	30
5	Unloading	

(c) Aging:

After mixing, the mixture is allowed to stay for minimum 16 hour and Maximum for 4 Days for aging in controlled atmosphere of 25⁰C and 50% Relative Humidity. This helps for polymerization of carbon to take place by carbon- carbon interlocking mechanism. The Mixture is then Sieve with 3.5 mesh Size so that only coarser and less than coarser particle can pass through it. The mixture properties is then checked so that its volatile content should be in the range of 1.35-1.45 and compressive height after applying a load of 10 ton should be above 31mm. the bar form after pressing has been shown in figure 4.1

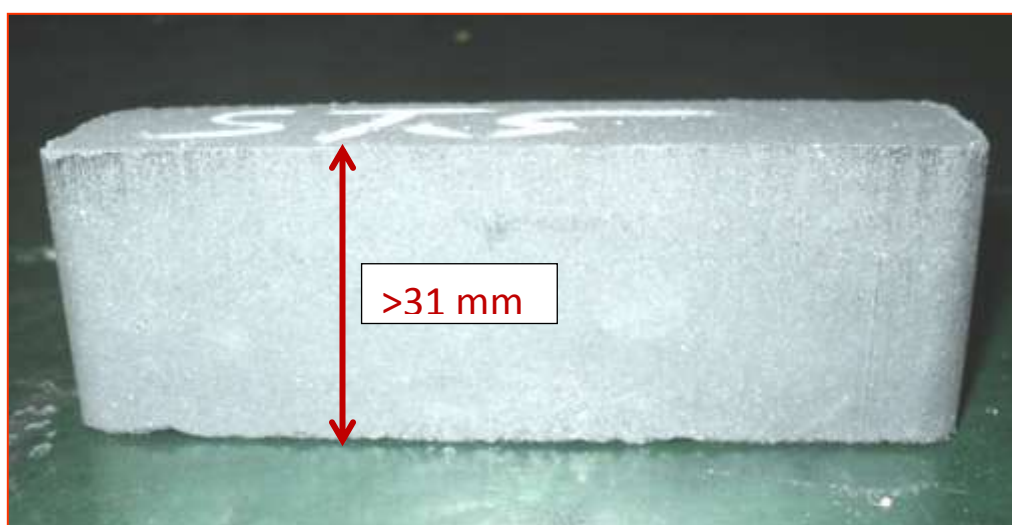


Fig 4.1 Bar showing compression height after aging

(d) Molding and Pressing:

A cylindrical Rubber mold of diameter 150 mm and height 200mm is filled with mixed material. In order to avoid sticking of the material the mandrel is coated with kerosene. Vibration Pressing is done after filling the mold. Vibration of mold is done so that the material will settle down in the mold and high packing can achieve within shortest possible time. Molding and pressing has been shown in figure 3.2



Fig 4.2 (a)Mold after filling the raw material. (b) vibration pressing during mold filled up

(e) Cold isostatic Pressing:

Cold isostatic press is a molding device that provides homogeneous hydrostatic pressure over the entire surface of a rubber mold filled with powder. This method, also referred to as a hydrostatic press or a rubber press method, it is a materials processing technique in which high fluid pressure is applied to a powder part at ambient temperature to compact it into a predetermined shape. The powder part is consolidated into a dense compacted shape which leads to a reduction of internal stresses, eliminating cracks, strains and laminations so that component produced after CIP are free from Cracking and warping during firing. Water or oil is usually used as the presser medium. In this project an cold isostatic pressure of 1000 bar is applied on the mold for 4 minute soaking time with total cycle time of 25 min. CIP is used to makes complex shapes, and to press more than one shape at the same time.

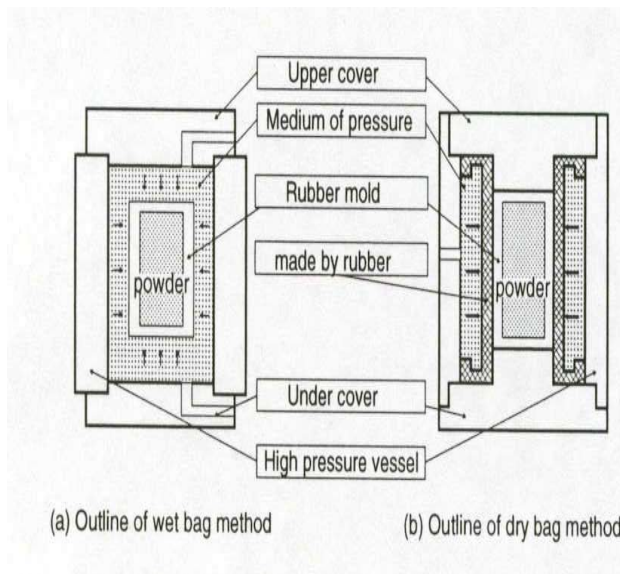
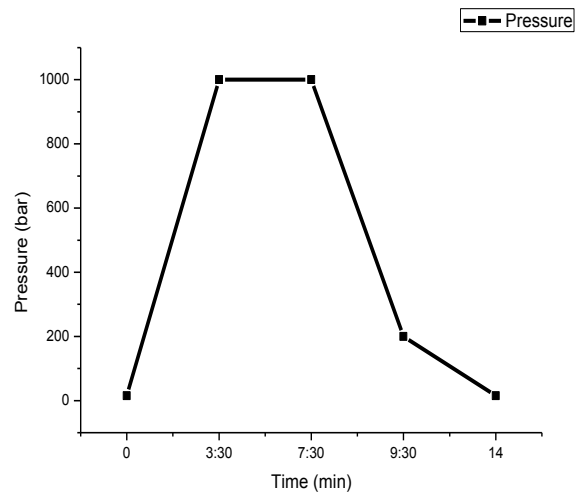


Fig 4.3 (a) Cold isostatic Presser



(b) pressing schedule

(f) Curing:

The carbon materials are impregnated using the vacuum-pressure process. Optimum impregnation of porous carbon and graphite articles is to reduce their gas permeability and increase their strength. Curable Resin mainly Phenolic can be used as impregnating agents. Impregnation is carried out in vacuum chamber and then applying pressure differences of upto 10 bars. The curing program and exposure to heat must be adjusted to ensure that the impregnating agent does not leak out of the porous system and thus reduce the impregnating effect.

Variations in the behaviour of phenolic resin with temperature are given below

At 70-80°C: A fused mass with changing viscosity develops, and liquid substances begin to vaporize.

At 110-120°C: the hexamethylene tetramine in novalak- hexa systems begins to decompose, initiating curing of the novalak and leading to liberation of ammonia (gas evolution) and a rise in viscosity.

At 170-180°C: the Resin system undergoes essentially complete crosslinking to yield a three- dimensional polymeric arrangement, and consolidation of the structure takes place.

At 180-200°C: Cleavage of benzylamine moieties in the cured phenolic novalak leads to further, relative minor evolution of ammonia and to additional attachment of the strength and thermal stability.[20]

Slow Heating Rate of 0.75°C/min till temperature reached 270°C and then the soaking period is of 5 hrs.



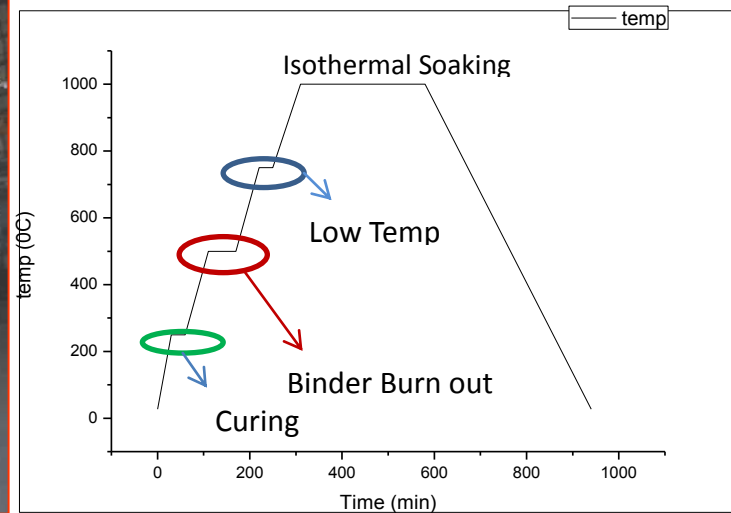
Fig 4.4 shows curing furnace

(g) Coking:

Refractories are coked at reducing atmosphere to develop the materials refractory properties. The cured samples pass through a heat treatment, which results in a thermally stable refractory and or crystallization. In present work sample are coked till 1000°C with rising time of 5hrs and at 1000°C soaking time is 3hrs followed by controlled cooling of 6hrs till room temperature is reached.



Fig 4.5 (a) shows Bell crank furnace



(b) coking schedule

Binder Burn Out:

Removal of volatile material such as absorbed water and the conversion of additives such as metal, organic compound or organic binder takes place. Heating Rate should be less than 2°C because rapid heating may cause Boiling and evaporation of organic additives leading swelling and even cracking of the suspension. Typical the holding temperature in this stage is 400°C - 500°C

Low temperature Soak:

Promote chemical Homogenisation or the reaction of powder component. The hold temperature is commonly below that for the Onset of measurable coking.

Heating up to the coking temperature:

For large bodies the heat up times can stretch for many hrs to avoid temperature gradient that could lead to cracking, or to avoid the formation of dense outer layer on an incompletely densified core.

Isothermal Soaking:

Higher Soaking temperature leads to faster densification but rate of coarsening also increases. The increased coarsening Rate may leads to Abnormal grain growth were pores are trapped inside large grain.

4.3 General Characterization:

4.3.1 Apparent porosity (AP) and Bulk density (BD) :

AP was measured as per the standard of IS: 1528, Part-8(1974) both for tampered and coke samples. The Archimedeian evacuation method generally measures both bulk density and apparent porosity.

AP is defined as ratio of the total volume of the closed pores to its bulk volume and expressed as a percentage of the bulk volume. Closed porosity are the pores that are not penetrated by the immersion liquid, whereas open porosity are the those pores which are penetrated by the immersion liquid.

The test specimen of 40 mm × 40mm × 40 mm were taken and after taking the dry weight(i) the specimen were boiled for 2 hours. This process is planned to fill up all voids present in the specimen with water. Then the suspended weight(W) and soaked weight (S)were taken.

$$\text{Apparent porosity} = (s - w / s - i) * 100 \quad (1)$$

Bulk density (BD) is defined as the ratio of the mass of the dry material of a porous body to its bulk volume. It is usually expressed in gm/cc.

$$\text{Bulk Density} = \left(\frac{w}{s-i} \right) * \eta \quad (2)$$

where,

s - weight of soaked piece

w - weight of dry piece

i - weight of the piece soaked and immersed

η -density of fluid

4.3.2 Cold Modulus of Rupture (ASTM C-133):

The cold modulus of rupture of a refractory material indicates the flexural strength and its suitability for use in construction. It is indicative of the strength of the bonding system of the refractory product. Strengths of refractories are usually reported in terms of the three-point bend strength or the flexural strength, frequently called the modulus of rupture (MOR). In the case of refractories, there exists a standard test for this simple strength measurement. It is based on the familiar formula:

$$\sigma(\text{MOR}) = \frac{3PL}{2bh^2}$$

where

$\sigma(\text{MOR})$ is the strength in three-point bending

L is the length of the test span

b is the specimen width

h is the specimen height.

P is the fracture load

4.3.3 Thermal Shock Resistance /Spalling Resistance:

According to Definition (IS:4041-1967) the Cracking or Fracture of Refractory Product Caused by Differential Expansion due to thermal Shock a steep Temp Gradient, a crystalline conversion or a change in composition near hot face

The specimen of Size 50 ± 2 mm in the form of a square with 75 mm height were first coated with the high temperature material then the specimen were kept for drying for 10 hours followed by air cooling. Then the sample were initially kept in the furnace maintained at 1200°C for 30 min followed by sudden air quenching for 10 min after that sample were again kept in furnace for 10 min then again suddenly brought down to ambient condition by cooling it in air for 10 minutes. The number of cycles before any crack in the specimen was noted down as the spalling resistance.

4.3.4 Corrosion/erosion resistance

A concentration gradient occurs in the refractory composition at the boundary region when the refractory comes in contact with the molten slag. The refractory components diffuse through the interfacial film and dissolve in the liquid. The interfacial film influences the rate of dissolution. The larger the concentration gradient, the faster the dissolution rate and thus the refractory dissolves more readily.

Since the exposure of refractories to molten metal/slag is a dynamic process, the tests simulating the conditions also need to be dynamic. For steelmaking refractories, the rotary slag test (ASTM C874) provides close simulation of the conditions in steel-making refractories.

Rotary Drum Test

Sample of dimension 150×40×40mm were cut from each batch. The samples are then coated with high temperature coating material followed by drying inside dryer for 10 hour. Then about 10 samples were lined inside the sample holder by using magnesite clay for setting purpose. Then after drying in room temperature the drum was fitted to the rotary drum machine. Prior to the start of testing, the apparatus was connected to gas cylinders (LPG+ Oxygen) and the pressures of gas of both cylinders are maintained at 4 Kg/cm². Speed of the rotating drum maintained at 5 rpm. Before the start of testing with slag and metal, the samples were preheated at 1000⁰C for 1 hour. Then 50wt% metal and 50wt% LD slag were put inside the sample holder. Simultaneously the temperature was increased to 1550⁰ C by increasing the gas pressure and fuel supply. The temperature was kept constant at 1550⁰ C for 30 min. The temperature of testing was observed by means of pyrometer. After 30 minutes of testing, the molten metal and slag was tapped out from the machine and fresh slag and metal again added to it for further testing. Similarly, another tapping was done after 30 minutes. After 2 nos. of tapping, the test was stopped and after cooling the eroded samples was taken out of the rotary drum and the eroded depth was measured by means of slide calipers. The testing was done on the basis of ASTM C-874. The chemical composition of LD slag has been given in table

Table 4.13 Chemical composition of LD Slag

C	Si	P	S	Mn	Al
0.06	0.02	0.3	0.02	0.3	0.04



Fig 3.6 Rotary Drum Testing Machine

4.3.5 Microstructure Analysis:

Thin slice of sample were cut from the specimen and kept it for drying for 2 hours. Prior to microstructure analysis the sample were coated in order to make the specimen electrically neutral so that clear SEM analysis can be done. Then the microstructures of these samples were done using scanning electron microscopy (SEM, model JSM 6480 LV JEOL, Japan).

4.3.6 X-Ray Analysis

X Ray analysis can be done with the help of X-ray Diffractometer (Philips PANalytical, Netherland) machine. The instrument Parameters are given below:

Voltage/Current – 35kV/25mA

Incident beam slit – 0.25 mm

Divergence beam slit – 0.5 mm

Radiation - Cu-K α , $\lambda = 1.54056\text{\AA}$

Filter – Nickel

The samples that are fired at a temperature about 1000°C and corroded samples (testing at $1550^{\circ}\text{C}/1\text{ hr}$) were first broken into pieces. These pieces are then grounded into fine powder for XRD analysis.

4.3.7. BET Analysis:

In order to determine the surface area of the nano carbon material BET analysis has been done. For BET analysis liquid nitrogen has been used to cover the surface area of the particles. BET analysis has been done on quanta chrome machine

4.3.8 Shear Stress:

Shear stress is the resistance offered by one layer of refractory to the other. This stress has been calculated in order to determine the resistance offered to inner surface by its subsequent layer.

$$\tau = \frac{3w}{4bh}$$

Modulus of Elasticity: Modulus of Elasticity is the amount of stress for unit deformation. Modulus of Elasticity has been calculated by

$$\text{Modulus of Rupture} = \frac{\sigma}{\varepsilon}$$

CHAPTER 5 RESULTS AND DISCUSSION

5.1 The effect of fixed carbon (FC) percentage of graphite on Zirconia-Graphite refractory

In present work, first the effect of different fixed carbon (FC) percentage of graphite on physical, thermal and mechanical properties of zirconia-graphite refractory has been studied. Flake Graphite with fixed carbon percentage (99% FC, 94% FC and 80% FC) was used as filler materials. Different size fraction of zirconia particles was chosen (shown in Table 5.1) in order to achieve a better compaction in green bodies during fabrication. The amount of Ca stabilized zirconia was 82 wt% and amount of different graphite was fixed to 18 wt%. The size fraction of zirconia used was also kept constant. Silicon was added to zirconia-graphite mix as an antioxidant and novalak resin in both powder and resin form was used as the binder. The percentage of silicon antioxidant was kept at 0.5 wt % of the total batch and the amount of resin binder was 12 % of the batch. 50% of the resin binder was used in the powder form and rest was in the liquid form. The amount of antioxidant and resin binder was kept constant through out the work. For each batch three samples were prepared. After mixing of all ingredients, samples were shaped and compacted by Cold Isostatic Pressing method. All samples were cured at 277°C for 10 hours to initiate polymerization of resin binder. During curing loss of volatile matter content also takes place. After curing samples were fired at 1000°C in reducing atmosphere for 10 hours. The fired samples were then subjected to different property testing (Table 5.1).

Table 5.1. Batch formulation of Zirconia-Graphite refractory with varying fixed carbon percentage.

Chemical composition		Composition 1			Composition-2			composition-3		
	Size Fraction									
CaO stabilized ZrO ₂	Coarser	23.8			23.8			23.8		
	Medium	32.7			32.7			32.7		
	Fines	25.5			25.5			25.5		
Graphite	99% FC	18			-			-		
	94% FC	-			18			-		
	80%FC	-			-			18		
		12			12			12		
Resin Binder		0.5			0.5			0.5		
Antioxidants										
Trial		T-1	T-2	T-3	T-1	T-2	T-3	T-1	T-2	T-3
Apparent Porosity(%)		21.5	17.9	18	20.2	23.1	21.1	22.8	23.3	21.1
Bulk Density(gm/cc)		3.15	3.25	3.26	3.22	3.09	3.14	3.13	3.11	3.17
MOR(Kg/cm ²)		76	73	74	70	65	70	65	68	68
Shear stress(Kg/mm ²)		7.6	6.16	6.43	7.11	6.86	6.9	6.9	7.4	7.91
Corrosion Resistance*, width loss(mm)		15.7	20.36	17.81	17.18	20.74	19.11	21.81	24.19	20.55

*Corrosion resistance test was carried out in Rotary Drum Method with metal and slag [basicity (C/S) = 3], at temperature 1550⁰C±50⁰C, metal and slag were replaced 2 times during one run.

Dilatometry Test:

Generally, the strength of zirconia-graphite refractory comes from carbon interlocking due to polymerisation of resin. Sintering of zirconia particles is purposefully avoided due to requirement of high temperature, which would lead to loss of carbon from refractory. Dilatometry study has been carried out for the samples to determine the maximum possible temperature up to which specimen could be fired without sintering.

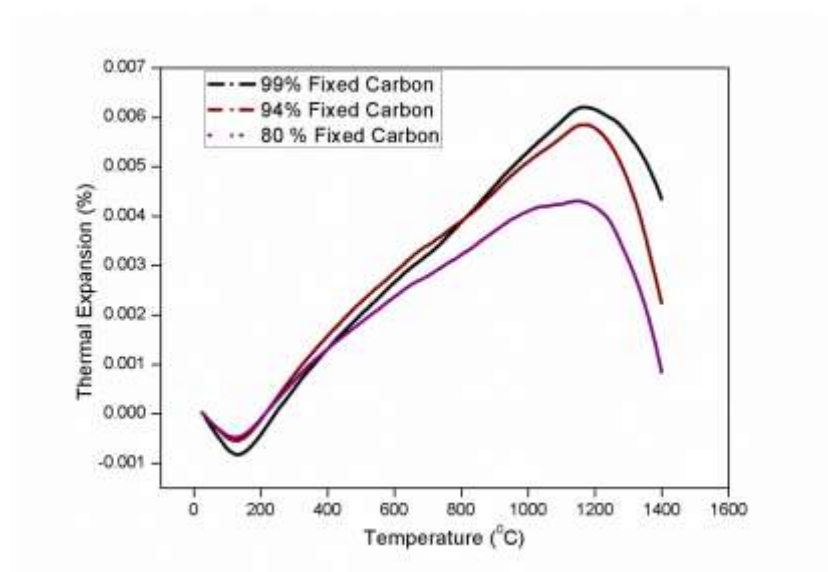


Figure 5.1 Thermal Expansion behaviour as a function of Fixed carbon

It has been observed from the figure that sintering initiates at around 1100⁰C for refractory containing 80% FC graphite. For refractory containing 94% FC graphite and 99% FC graphite sintering initiates at the same temperature i.e. around 1100⁰C. It can be said from the observation that graphite content as well as fixed carbon content has particularly no effect on the sintering temperature. The firing temperature for the samples has been fixed to 1000⁰C lower than the sintering initiate temperature i.e 1000⁰C to avoid any kind of carbon loss from the refractory.

Phase analysis (XRD):

XRD pattern of zirconia-graphite refractory samples after firing has been shown in Fig. 5.2 Cubic zirconia and tetragonal zirconia phase has been identified as a major phase with small quantity of monoclinic phase. It could be seen from the XRD pattern that as the purity of graphite decreases the intensity of carbon peak decreases which reveals that the percentage of carbon present in the zirconia-graphite refractory has reduced.

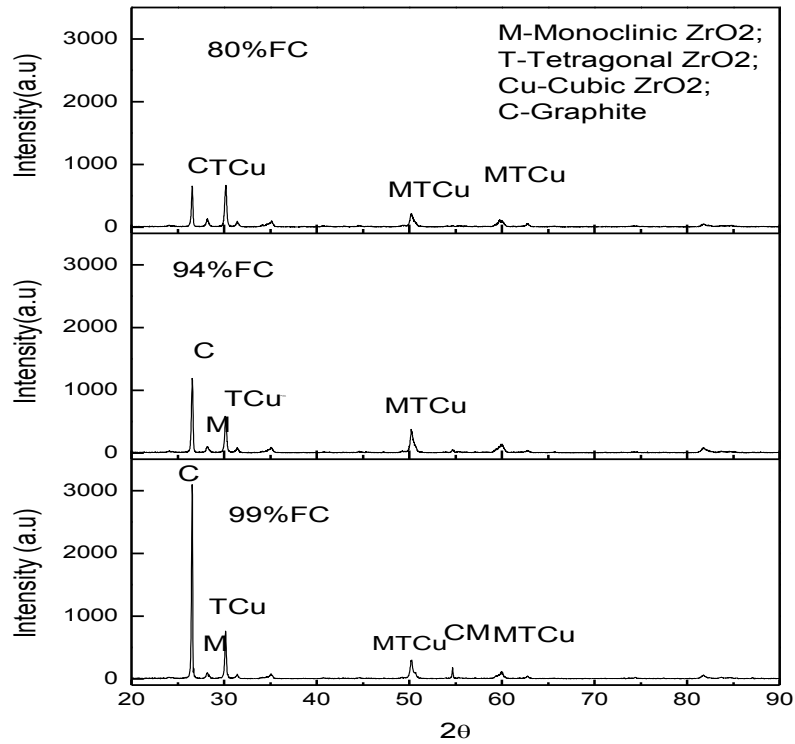


Fig 5.2 XRD pattern of zirconia-graphite refractory with 80%FC graphite, 94%FC Graphite,99%FC graphite

5.1.1 Variation of Apparent porosity (AP) and Bulk Density (BD) of zirconia-graphite refractory with Fixed Carbon percentage of graphite.

Apparent porosity (AP) of the Zirconia–Graphite refractory (fired at 1000⁰C) as a function of fixed carbon percentage of graphite has been plotted in Fig 5.3

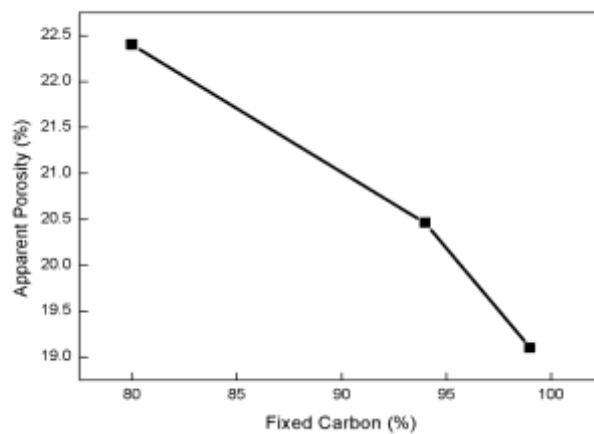


Fig 5.3 Apparent Porosity as a function of Fixed Carbon

From the Fig. 5.3, it has been observed, that there was a gradual decrease in apparent porosity with the increase in fixed carbon percentage of flake graphite. The AP of the samples decreases from 22.8% to 20.2% as the purity of graphite increases from 80% to 99%. It could be due to the fact that 99% FC graphite has less amount of volatile matter content. As the 80% FC containing graphite has high volatile content which vaporised during coking, thus leaving behind the pores, hence the apparent porosity increases as the percentage of fixed carbon present in the graphite decreases.

Bulk Density of the Zirconia–Graphite refractory (fired at 1000⁰C) as a function of fixed carbon percentage of graphite (fired at 1000⁰C) had been plotted in Fig. 5.4.

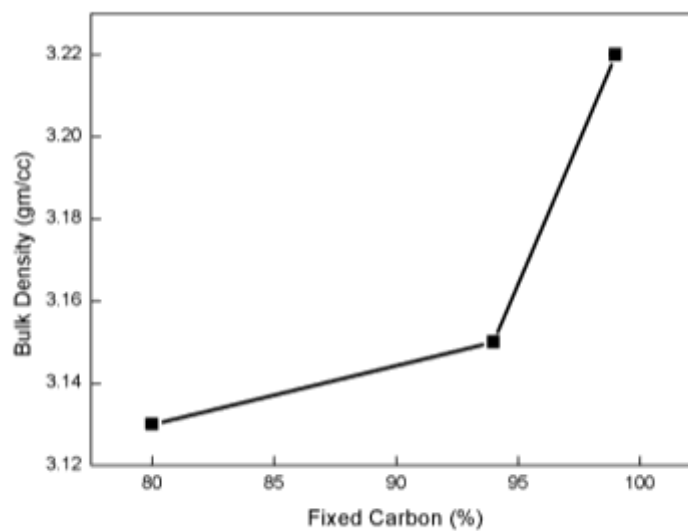


Fig 5.4 Bulk density as a function of Fixed Carbon

From the Fig. 5.4, it has been observed that bulk density increased as percentage of fixed carbon present in the graphite increased. The bulk density increases from 3.13 gm/cc to 3.22gm/cc as the percentage of fixed carbon present in the graphite increases from 80% to 99%. Again, it could be attributed that 99% FC containing graphite has less volatile content as compared to 94% and 80% FC containing graphite. 80% graphite has high volatile content which vaporised during coking leaving behind the more pores leading to more porosity and less bulk density.

5.1.3 Variation in Mechanical properties of zirconia-graphite refractory as a function of fixed carbon percentage of graphite.

5.1.3.1 Cold modulus of Rupture

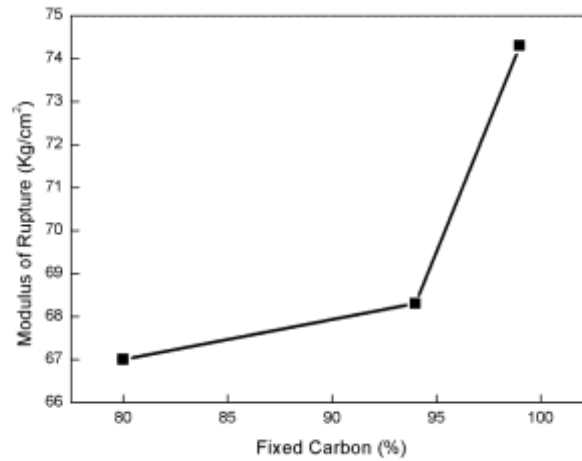


Fig.5.5 Cold Modulus of Rupture as a function of fixed carbon

It has been observed from the figure that the cold modulus of rupture (CMOR) is gradually increasing as the FC content of the graphite is increasing. CMOR values has increased from 65MPa to 76MPa as the percentage of FC has increased from 80% to 99%. It could be related with the bulk density of the material. As we had observed that bulk density increases as the purity of graphite increases thus resulting in more particles compaction. High compaction and less porosity in the refractory samples lead to high strength to the specimen thus resulting in higher Modulus of rupture.

5.1.4 Slag Corrosion resistance behaviour of zirconia-graphite refractory as a function of Fixed carbon percentage of graphite in terms of width loss

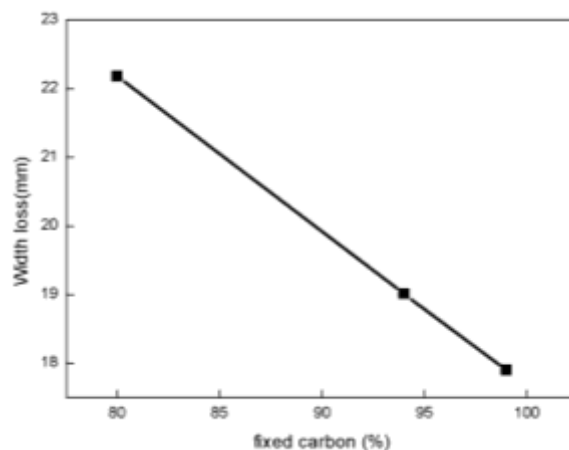


Figure 5.6 Slag Corrosion Resistance as a function of Fixed carbon

It has been observed from the figure that slag resistance of the Zirconia-graphite increases as the percentage of fixed carbon in the graphite increases. It could be related with the anisotropic nature of the graphite. The carbon molecules at the surface in the graphite flakes are held together by covalent bond and therefore, having low free energy compared to the edges. At high temperature this anisotropic behaviour weakens leading to increase in the oxidability, thus leading to poor resistance against slags. The retention of the anisotropic behaviour increases with the purity of graphite. Therefore, 99% fixed carbon graphite may have very low free energy. Therefore, their reactivity and their wettability in the molten metal and liquid slags are very low. Therefore, refractory with graphite containing 99% FC showed better slag corrosion resistance compared to graphite having 94% and 80% FC.[48]

5.1.5 Thermal Expansion Behaviour of Zirconia Graphite Refractory:

Spalling Resistance:

Spalling resistance has been carried out by small prism test (air quenching) method. All the samples were tested for 15 cycles. It has been observed that No crack was found till 15 cycles. It could be related with the thermal conductivity of the graphite. As the percentage of fixed carbon present in the graphite increases, these carbon promotes high thermal conductivity as a results graphite easily promotes the transfer of heat from hotter side to cooler side. Thereby, reducing the temperature gradient present inside the refractory wall. Thus, the thermal shock profile generated in the refractory body gets reduced which results in an excellent ability to absorb the mechanical stress due to the thermal expansion and shrinkage.

5.1.6 Scanning electron microscopic image:

The micro structure of zirconia-graphite refractory with graphite having 99% FC, 94% FC and 84% FC are shown Fig.5.7. The samples were fired at 1000⁰C in reducing atmosphere. It can be observed that in case of 99% FC containing graphite, the flaky nature of graphite is retained in the refractory. This could be the reason for having better thermal spalling resistance in the refractory. Pores were also observed in the samples. For 94% FC containing graphite, it has been observed that flaky nature of the graphite was retained in the sample. For 80% FC containing graphite, the flaky nature of the graphite is not so well maintained. More number of pores can also be observed in the samples. The poor spalling resistance as well as poor corrosion resistance of 80% FC containing graphite may be due to destruction of graphite structure in the refractory.

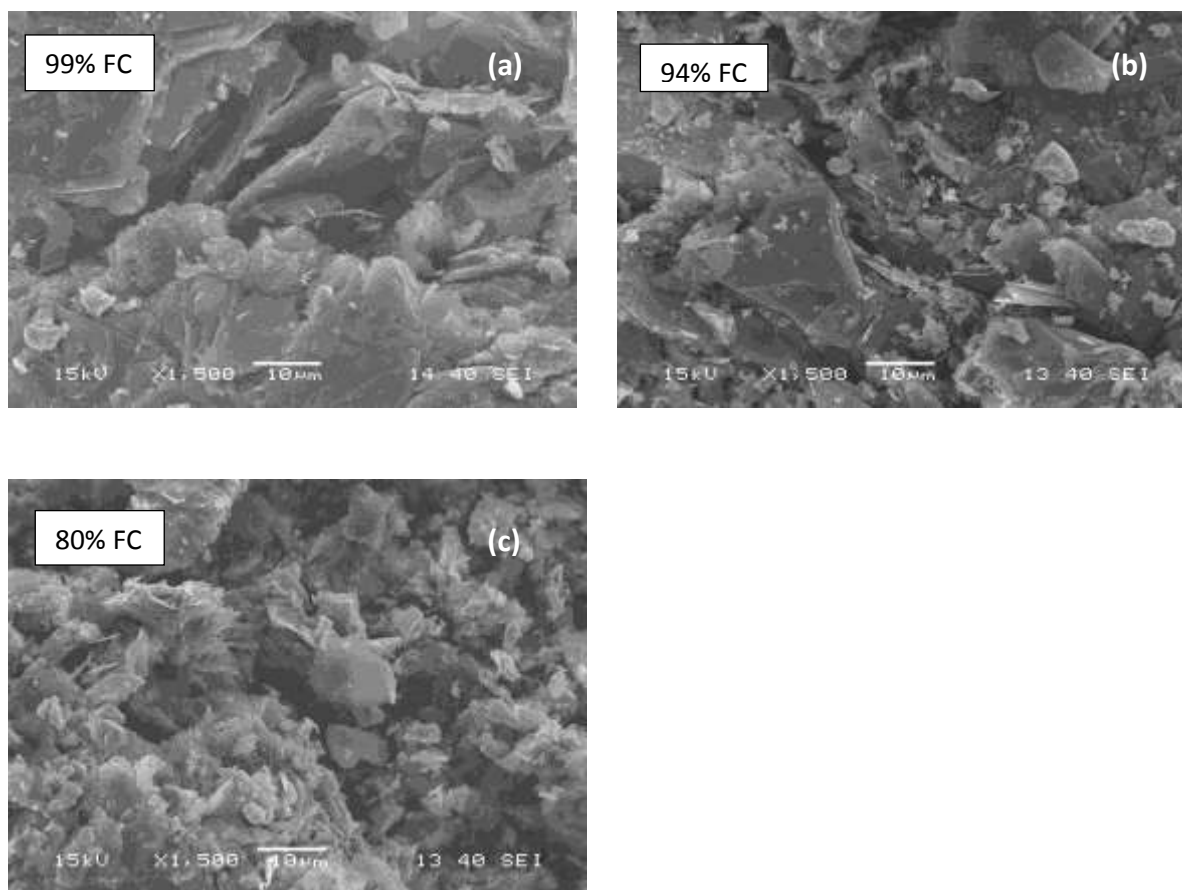


Fig.5.7 Scanning electron Microscopic image of (a) 99% Fixed carbon graphite (b) 94% Fixed carbon graphite (c) 80% Fixed carbon graphite in Zirconia-graphite refractory

Summary:

Studies on zirconia-graphite refractory with the variation in fixed carbon percentage of graphite, suggested that refractory prepared with 99% FC showed enhanced physical, mechanical and thermal behaviour as compared to 94% FC and 80% FC containing graphite. 80% FC containing graphite refractory showed most deteriorated in properties. Therefore, further study with 80% FC has been discarded. To improve thermal spalling resistance as well as corrosion resistance, it has been decided to replace some amount of graphite with other form of carbon and to study the effect on thermal mechanical and corrosion resistance properties of zirconia-graphite refractory. As a first step, it has been decided to replace 2% of graphite with amorphous carbon black (ACB) for 99% FC and 94% FC graphite while keeping other composition and processing parameter same as before. This study has been done in order to determine whether amorphous carbon black could be a potential candidate to enhance thermal spalling resistance as well as corrosion resistance.

5.2.1 Batch formulation of amorphous carbon Black on the zirconia-graphite refractory: carbon Black. Raw material used in the formulation of zirconia graphite refractory is same as in previous section 5.1 The zirconia-graphite refractory has been prepared by replacing 2 wt% graphite with amorphous carbon black (ACB). Batch composition of zirconia-graphite refractory has been shown in table 5.2

Table.5.2 Batch composition of Zirconia-graphite refractory by inclusion of Amorphous carbon Black.

Raw Material(wt%)		T-4	T-5
CaO stabilized ZrO ₂	Coarser	23.8	23.8
	Medium	32.7	32.7
	Fines	25.5	25.5
Graphite	99% FC	16	-
	94% FC	-	16
Amorphous carbon Black		2	2
Additives		12	12
Antioxidants		0.5	0.5
Apparent Porosity(%)		21.3	22.2
Bulk Density(gm/cc)		3.13	3.14
Modulus of Rupture(Kg/mm ²)		66	66
Shear stress(Kg/mm ²)		6.81	6.81
Width loss(mm)*1		19.12	24.19

**Corrosion resistance test was carried out in Rotary Drum Method with metal and slag [basicity (C/S) = 3], at temperature 1550⁰C±50⁰C, metal and slag were replaced 2 times during one run.*

Dilatometer Test:

Generally, the strength of zirconia – graphite refractory comes from carbon interlocking due to polymerisation of resin. Sintering of zirconia particles is purposefully avoided due to requirement of high temperature, which would lead to loss of carbon from refractory. Dilatometry study has been carried out for the samples to determine the maximum possible temperature up to which specimen could be fired without sintering.

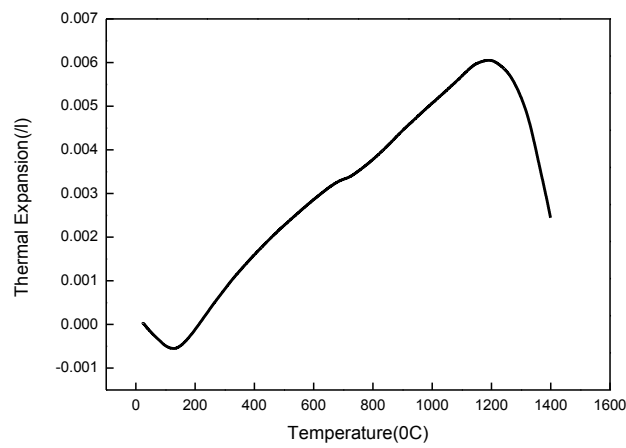


Fig.5.8 shows Thermal Expansion Behaviour as a function of 94%FC graphite with ACB

It has been observed from the figure that sintering initiates at around 1100⁰C for refractory containing 94% FC graphite with amorphous carbon Black. It can be said from the observation that graphite content as well as fixed carbon content has particularly no effect on the sintering. The firing temperature for the samples has been fixed to 1000⁰C lower than the sintering initiate temperature i.e 1000⁰C to avoid any kind of carbon loss from the refractory.

Phase Analysis:

XRD pattern of zirconia-graphite refractory samples after firing has been shown in fig. Cubic zirconia and tetragonal zirconia phase has been identified as a major phase with small quantity of monoclinic phase.

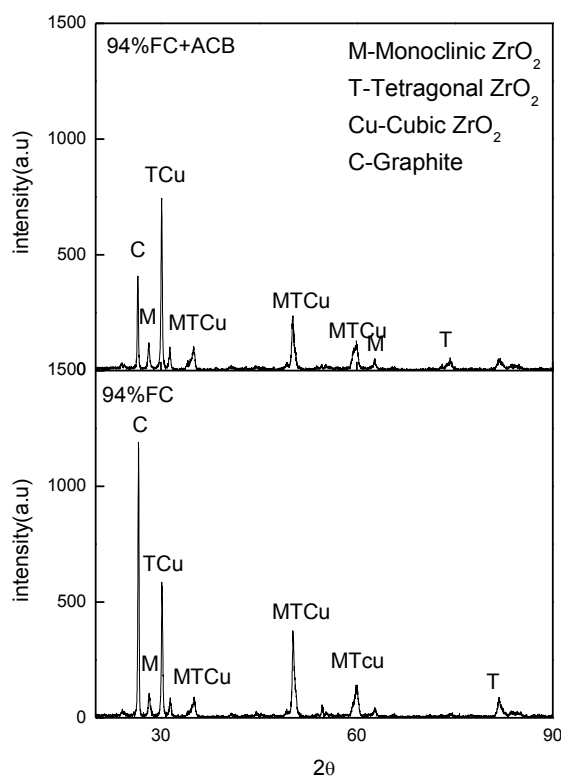


Fig.5.9. XRD pattern of 94% graphite with ACB and 94% graphite without ACB

It had been observed from the XRD Pattern that intensity of carbon peak present in the zirconia-graphite refractory containing 2 wt% ACB and 16wt% graphite was less intense compared to 18wt% graphite alone for same grade of graphite i.e 94% FC containing graphite.

Variation in Apparent porosity (AP) and Bulk Density (BD) of zirconia-graphite refractory as a function of Amorphous Carbon Black

Apparent porosity (AP) of the Zirconia–Graphite refractory (fired at 1000⁰C) as a function of Amorphous Carbon Black has been plotted in Fig 5.10

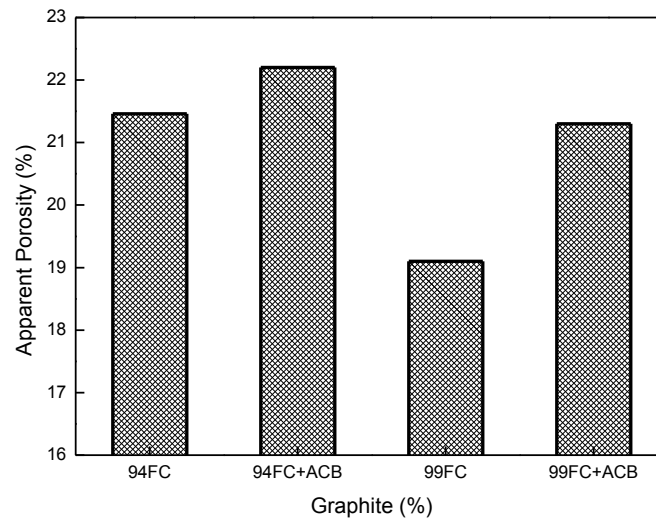


Fig.5.10 Shows Apparent Porosity as a function of Amorphous Carbon Black

From the Fig 5.10, it has been observed, that the Specimen containing ACB had apparent Porosity of 22.2% and 21.3% and that without ACB has 21.46% and 19.1% for 94% FC and 99% FC graphite containing refractory respectively. Thus the refractory in which ACB replaces graphite resulted in higher apparent porosity compared to that without addition of ACB. containing sample. It could be due to the fact that refractory in which ACB had replaces graphite had lower carbon content after coking, which had been observed from carbon intensity peak in XRD. Thus amorphous carbon black has higher free energy compared to graphite, therefore, it sublimate at higher temperature leaving behind the porosity. Thus the refractory in which 2wt% ACB has replaced graphite has higher apparent porosity than refractory without ACB.

Bulk Density (BD) of the Zirconia–Graphite refractory (fired at 1000⁰C) as a function of Amorphous Carbon Black has been plotted in Fig 5.11

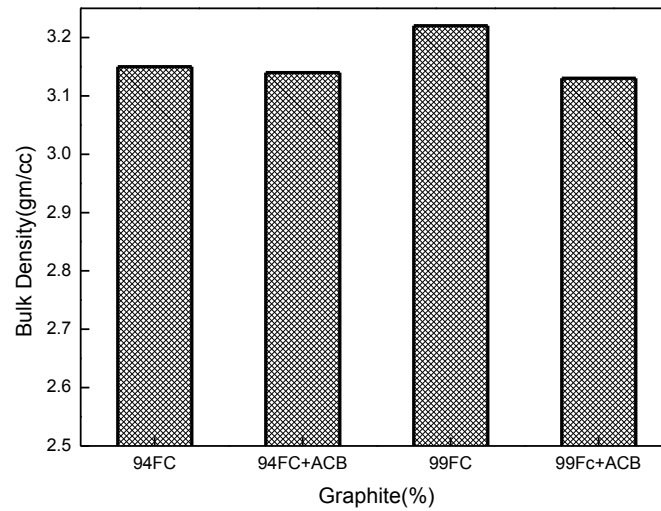


Fig.5.11 shows Bulk Density as a function of Amorphous Carbon Black

From the Fig.5.11, it has been observed the Specimen containing ACB has Bulk Density of 3.13gm/cc and 3.14gm/cc and that without ACB has 3.15gm/cc and 3.22gm/cc for 94% FC and 99% FC graphite containing refractory respectively. Therefore, the refractory in which ACB replaces graphite has lower Bulk Density compared to that without addition of ACB containing sample. As the apparent porosity of the ACB containing refractory were higher hence there was slight decrease in BD value.

5.2.3 Variation in Mechanical properties of zirconia-graphite refractory as a function of Amorphous Carbon Black

5.2.3.1 Cold modulus of Rupture

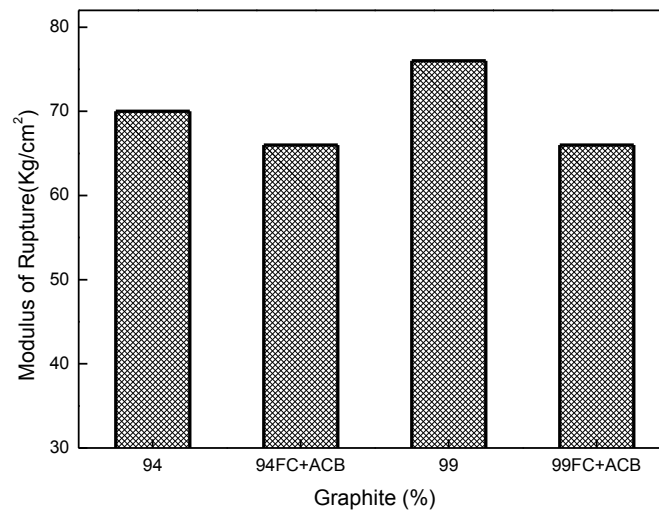


Fig5.12 Cold Modulus of Rupture as a function of Amorphous carbon Black

From the Fig.5.12, it has been observed the Specimen containing ACB had Cold Modulus of Rupture (CMOR) of 66Kg/cm² and 66Kg/cm² and that without ACB has 68.3Kg/cm² and 74.3Kg/cm² for 94% FC and 99% FC graphite containing refractory respectively. The refractory without ACB had higher bulk density hence the CMOR values were more for those refractory samples.

5.2.4.1 Slag corrosion resistance:

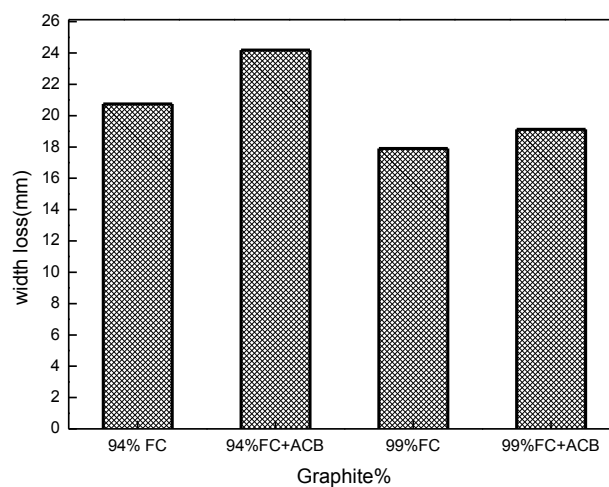


Fig. 5.13. Variation of width loss cause by slag as a function of Amorphous Carbon Black

The variation of width loss caused by the slag as a function of amorphous carbon black has been shown in figure 5.13. It has been observed from the figure that in zirconia-graphite refractory in which ACB replaces graphite has more width loss caused by the slag as compared to without addition of ACB. It could be due to ACB has higher free energy compared to graphite due to the amorphous nature of the carbon. This high energy had increased carbon reactivity at high temperature. Thereby, causing it to get oxidised and resulting in loosening of zirconia-graphite bond. Therefore, it was easy for the slag to penetrate into the zirconia refractory resulting in more width loss as compared to Zirconia-Graphite refractory without ACB. Moreover, ACB had high reactivity and high wettability. It could react with the slag present in the mold, thereby, having higher width loss as compared to ZG refractory without ACB.

Summary:

Studies on thermo-mechanical and corrosion properties of zirconia-graphite refractory where 2 wt% of graphite was replaced by amorphous carbon black (ACB) did not show any improvement. The properties were deteriorated for both the samples where FC percentage of graphite was different (i.e. 99% FC and 94% FC). Therefore, amorphous carbon black could not be considered as a potential replacement of graphite. In order to improve thermal spalling resistance as well as corrosion resistance, it has been decided to reduce the percentage of graphite from refractory and addition of nano carbon in to refractory. Zirconia-graphite refractory would be prepared by taking 99% FC containing graphite as raw material as it had shown better thermo-mechanical as well as corrosion resistance properties. In the previous studies the graphite percentage was fixed to 18 %. Now, the graphite content would be 15%, 12 %, 9% and 6% keeping other composition and processing parameter constant. In addition, a fixed amount of nano carbon (0.5 wt%) would be added to every set of composition. Nano carbon had high specific surface area, its behaviour is as same as that of graphite, it can also act as filler material by filling the pores between the zirconia aggregates. Therefore, addition of nano carbon may increase the thermo-mechanical properties of the zirconia-graphite refractory. For this purpose, two types of nano carbon were chosen. They were differed by their specific surface area and other physical properties (Table 4.5, 4.6). This study also aimed towards the optimization of the percentage of graphite with nano carbon in zirconia-graphite refractory.

5.3.1 Batch formulation of Zirconia-Graphite refractory by decreasing Graphite percentage and inclusion of Nano carbon:

The graphite with 99% FC has been used as a base raw material and other raw material used in the formulation of zirconia graphite refractory were same as used in previous section 5.1. The zirconia-graphite refractory had been prepared by reducing the graphite percentage from 18wt% to 6wt% in a difference of 3% and there was inclusion of 0.5wt% of two types of nano carbon (N220 and N115). Batch composition for above study has been shown in table 5.3. and table 5.4.

Table 5.3: Batch formulation of Zirconia-Graphite refractory by decreasing graphite percentage and inclusion of Nano carbon (N220).

Raw Material		T-6	T-7	T-8	T-9
Chemical composition	CaO-ZrO ₂	85	88	91	94
	Graphite(99%FC)	15	12	9	6
	Antioxidant	0.5	0.5	0.5	0.5
	Additives	12	12	12	12
	N220	0.5	0.5	0.5	0.5
Particle Size Distribution of ZrO₂	Coarser	24.7	25.6	26.6	27.4
	Medium	34.1	35.3	36.5	37.7
	Fines	26	26.9	27.9	28.7
Apparent Porosity (%)		23.3	23.6	20.2	22.9
Bulk Density(gm/cc)		3.19	3.32	3.47	3.51
Modulus of Rupture(Kg/mm²)		70	64	75	66
Shear stress(Kg/mm²)		7.6	6.3	7.4	6.4
Modulus of Elasticity		6.35	4.8	4.0	4.7
Slag Resistance (width loss)*		22.78	15.33	18.62	21.72

*Corrosion resistance test was carried out in Rotary Drum Method with metal and slag [basicity (C/S) = 3], at temperature 1550⁰C±50⁰C, metal and slag were replaced 2 times during one run.

BET Analysis of N220: BET Analysis of Nano carbon N220 reveals that its surface area is 131.05 m²/gm. From surface area Particle size has been calculated as 20.25 nm

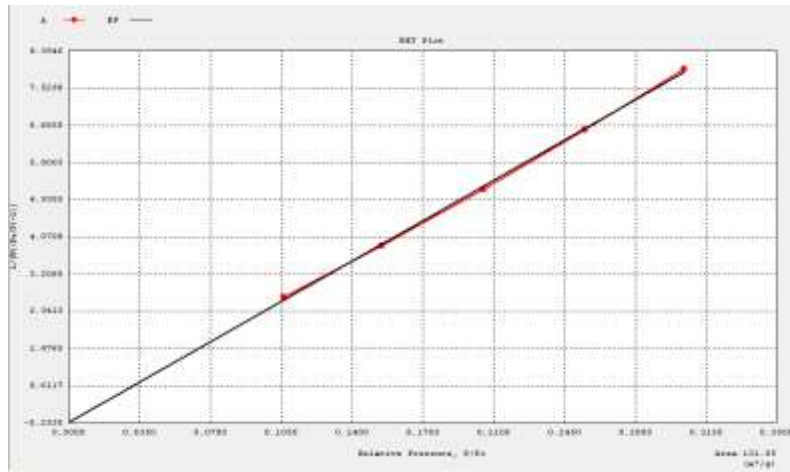


Fig5.14. BET Analysis of Nano Carbon N220

Table 5.4: Batch formulation of Zirconia-Graphite refractory by decreasing graphite percentage and inclusion of Nano carbon (N115).

Raw Material		T-12	T-13	T-14	T-15
Chemical composition	CaO Stabilized ZrO ₂	85	88	91	94
	Graphite(99%FC)	15	12	9	6
	Antioxidant	0.5	0.5	0.5	0.5
	Additives	12	12	12	12
	N115	0.5	0.5	0.5	0.5
Particle Size	Coarser	24.75	25.6	26.6	27.4
Distribution of ZrO ₂	Medium	34.1	35.3	36.5	37.7
	finer	26	26.9	27.9	28.7
Apparent Porosity (%)		23.3	23.4	19.1	24.1
Bulk Density(gm/cc)		3.19	3.31	3.45	3.57
Modulus of Rupture(Kg/mm ²)		68	69	77	78
Shear stress(kg/mm ²)		5.0	6.4	8.0	8.25
Modulus of Elasticity(GPa)		3.7	2.9	2.4	6.9
Slag Resistance (width loss)*		21.93	16.0	13.47	19.92

*Corrosion resistance test was carried out in Rotary Drum Method with metal and slag [basicity (C/S) = 3], at temperature 1550⁰C±50⁰C, metal and slag were replaced 2 times during one run.

BET Analysis of N115: BET analysis of Nano carbon N115 reveals that its surface area is 143.23 m²/gm. From surface area Particle size has been calculated as 18.53 nm

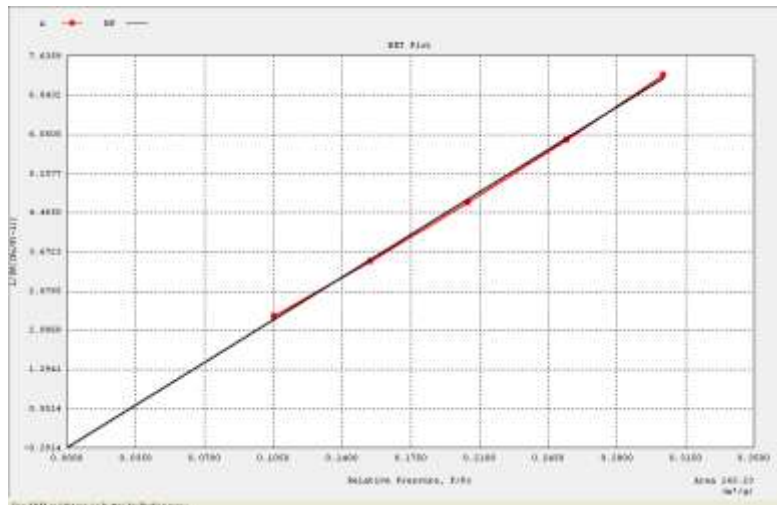


Fig 5.15 BET Analysis of N115

Variation in Apparent porosity (AP) and Bulk Density (BD) of zirconia-graphite refractory as a function of Nano Carbon Black

The variation of apparent porosity with decreasing graphite percentage and addition of 0.5 % Nano carbon has been shown in Fig 5.11. The samples were fired at 1000⁰C.

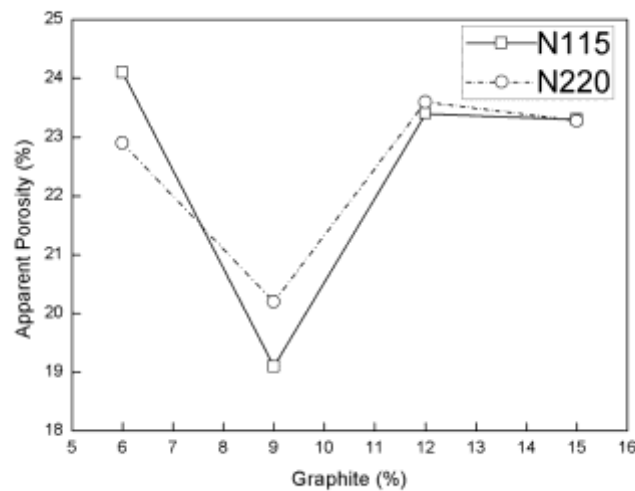


Fig.5.16 Apparent Porosity as a function of graphite

The variation of apparent porosity with graphite percentage has been shown in Fig 5.11. It has been observed from the figure that in zirconia-graphite refractory, with reducing the graphite percentage from 15% to 12%, apparent porosity did not change significantly. But there was a decrease in in apparent porosity when graphite percentage had been decreased to 9%. The value of apparent porosity was almost same as that of 18% graphite containing (99%

FC) samples. On further reduction of the graphite percentage up to 6wt% the apparent porosity increased due to higher concentration of zirconia in the sample. The increase in apparent porosity in the samples contain 12wt% graphite could be due to oxidization of nano carbon as well as some percentage of graphite. There could be free nano carbon which was not able to fill up all the pores in refractory matrix. For the samples containing 9 wt % graphite and 0.5wt% nano carbon, apparent porosity decreases. It could be due to the reason that nano carbon along with graphite had filled all the pores and were in correct proportion to cover the pores in zirconia matrix. Whereas, refractory containing 6wt% graphite along with nano carbon, high apparent porosity had been attained again. It could be due to the fact that graphite along with nano carbon were not sufficient to cover the pores in zirconia matrix. Therefore, nano carbon was not able to fill up the pores of the matrix and hence apparent porosity increases. Thus the optimum apparent porosity has been achieved in refractory containing 9wt% graphite and 0.5wt% nano carbon. Moreover, apparent porosity of N115 showed slight low value in comparison to N220 for every composition. As the specific surface area of N115 was higher than N220, therefore N115 nano carbon caused more efficient filling of the pores between the aggregates of the zirconia. Overall, the effect of nano carbon addition was successful in reducing the apparent porosity while there was decrease in graphite content. The minimum apparent porosity was obtained for the sample which had 9% graphite and 0.5% nano carbon with type N115.

5.3.2.2 Bulk Density

The variation of Bulk Density with decreasing graphite percentage as shown in Fig. 5.17

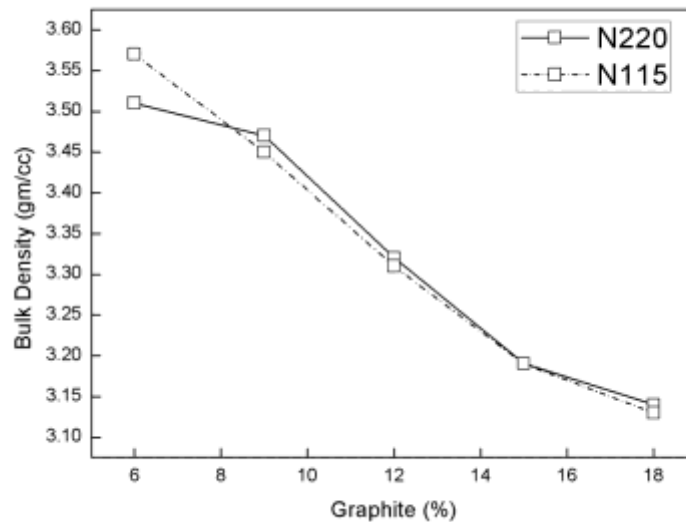


Fig. 5.17 Bulk Density as a function of Graphite

The variation in the bulk density of Zirconia Graphite refractory as a function of graphite content along with fixed nano carbon has been shown in Fig 5.17. It has been observed that with reducing the graphite percentage from 15% to 6%, bulk density increases from 3.13% to 3.57%. As graphite content was decreasing therefore, the zirconia percentage in the refractory was also increasing. Moreover, with increasing in nano carbon content the pores were also filled up. There was an increase in BD values when graphite content was reduced from 15% to 12%. This may be due to filling up of pores by nanocarbon. Same explanation may be given to the sample containing 9% of graphite. The increase in BD value was maximum for the sample containing 6% of graphite. This may be due to the higher percentage of zirconia present in the matrix. There was no significance change in BD value for two types of nano carbon. But, for the samples with 12%, 9% and 6 % graphite containing the BD values were greater than the samples with 18% graphite containing sample which had no nano carbon inclusion. So the increase in BD values may be due to two reason. First there was increase in zirconia concentration. Secondly, in Nano carbon effectively filled up the pores , hence increase in the BD values.

5.3.3 Mechanical properties of Zirconia-Graphite refractory by decreasing graphite percentage and inclusion of Nano carbon.

5.3.3.1 Cold modulus of Rupture

The variation of Bulk Density with decreasing graphite percentage as shown in Fig. 5.5

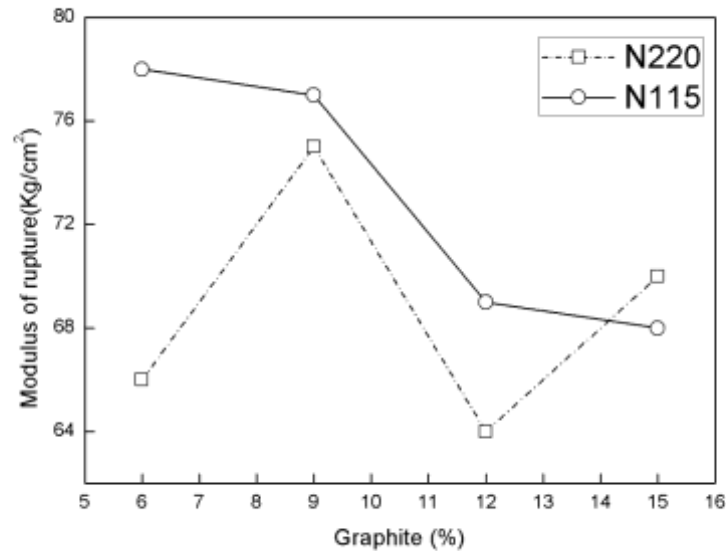


Fig. 5.18 Modulus of Rupture as a function of graphite and Nano Carbon Black

It was observed that cold modulus of rupture increased with decrease in graphite content. As the BD values were increasing with reducing graphite percentage, as well as zirconia concentration was also increasing with, hence there was increase in CMOR values. For samples containing nano carbon of type N 115, the CMOR values were greater than that of samples containing N220. These may be due to the lesser particles size of N115 which can effectively fill up the pores than N 220.

5.3.4.1 Slag corrosion Index:

Slag corrosion resistance of zirconia-graphite refractory as a function of graphite content has been shown in fig 5.19

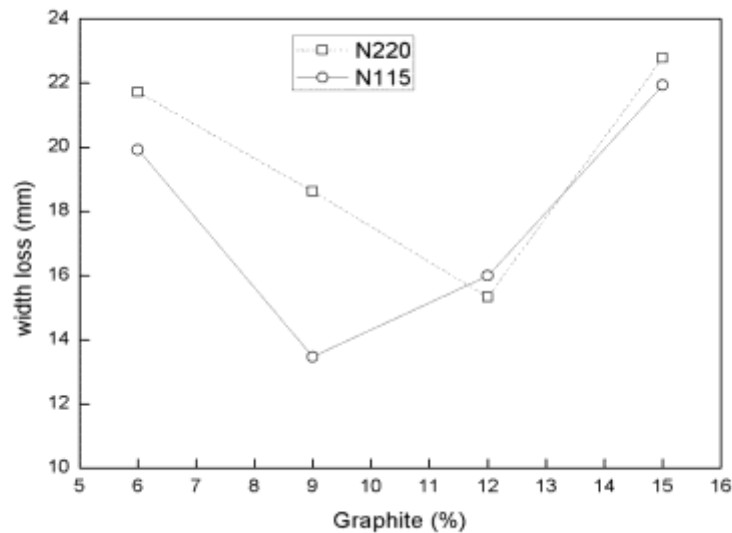


Fig 5.19 Width loss cause by the slag as a function of graphite and nano carbon

Slag corrosion resistance of N115 at every percentage of graphite is better than N220, it could be correlated with the iodine absorption number. Nano carbon is specified on the basis of Iodine absorption number, this is tendency of nano carbon to absorb iodine. The more the iodine absorption number the more the specific surface area of the nano particle. The iodine absorption number of N115 is $160\text{m}^2/\text{gm}$, which had higher iodine absorption number compared to N220 ($121\text{m}^2/\text{gm}$), which means that the N115 had high specific surface area as compared to N220. This high specific surface area helps the nano carbon to remain in the deflocculated state during mixing, thereby helping nano carbon to cover the grain boundary of zirconia and increase the non-wettability character of the zirconia-graphite matrix. Therefore, it prevented the attack of slag and they did not allow it to penetrate into the zirconia graphite refractory and prevent the corrosion of zirconia. Thus the slag resistance properties of N115 are higher than the N220.

Moreover, with decrease in the percentage of graphite and inclusion of both types of nano carbon, slag corrosion resistance of 9% graphite containing refractory was better than the other percentage of graphite. The nano carbon fills up the pores and did not allow the slag to penetrate. Hence there was increase in slag corrosion resistance. An anomaly could be

observed for refractory containing 9% graphite with 0.5% N220 nano carbon. The width loss was higher than 12% graphite containing sample. This may be attributed to some instrumental fault during experiment. For the refractory containing 6% graphite, the carbon present in the refractory was not able to cover pores in the zirconia matrix. Thereby, exposing the zirconia toward molten slag and allowed it to corrode the zirconia refractory.

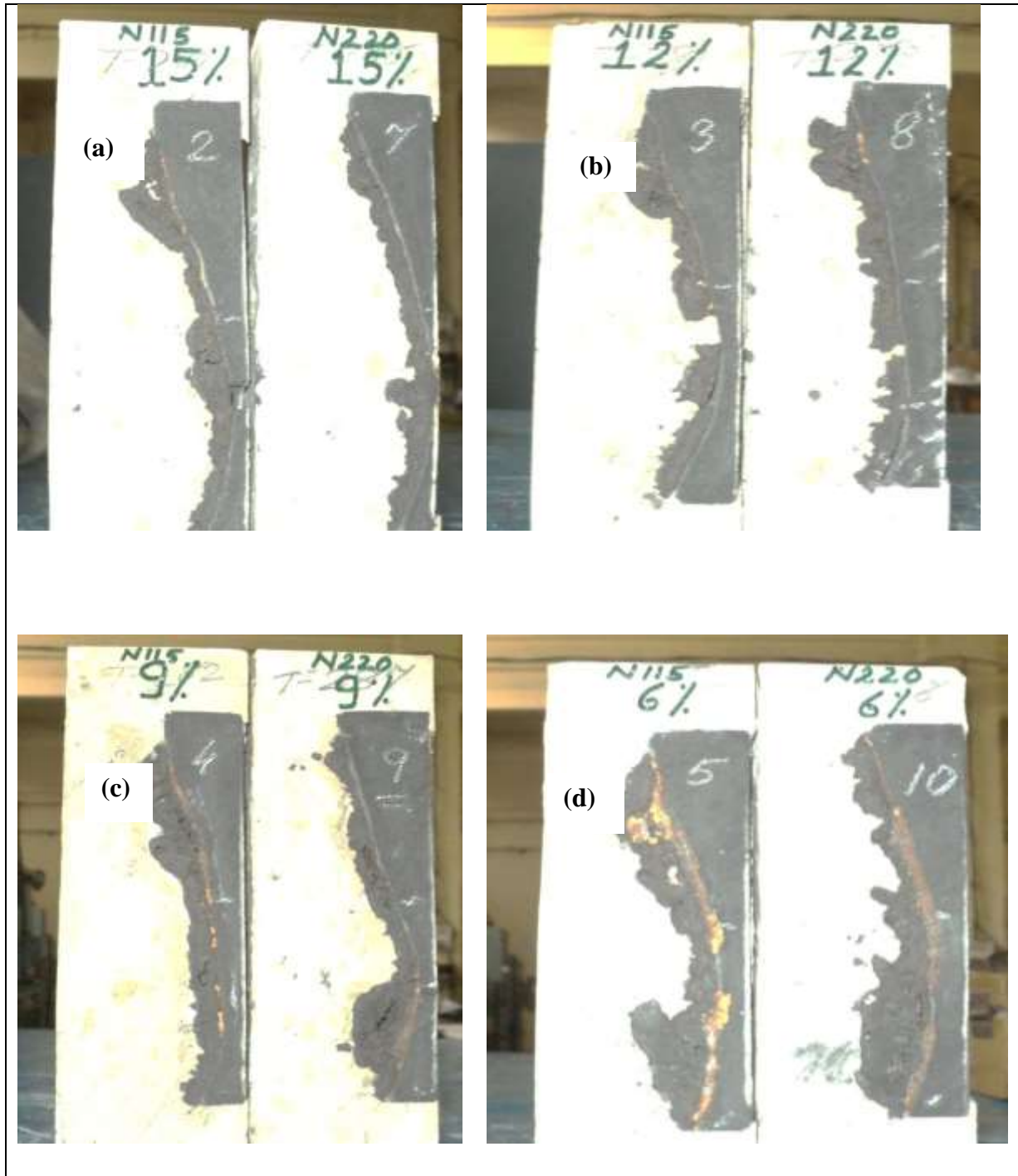


Fig. 5.20 Slag corrosion resistance, Comparing N115 and N220 for (a) 15% Graphite content (c) 12% Graphite content (d) 9% Graphite content (e) 6% Graphite content

5.3.4.2 Spalling resistance:

Thermal spalling resistant test of the Zirconia Graphite refractory as a function of graphite content has been shown in Fig:

It has been observed that every sample were able to withstand 15 cycles in small prism test of thermal spalling resistance done in air atmosphere. No crack was observed after 15 cycles. Again all refractory samples were tested for thermal spalling resistance in water quenching method. All samples withstand 15 cycles without any observation of crack.

The samples after spalling test by water quenching method were shown in Fig 5.21

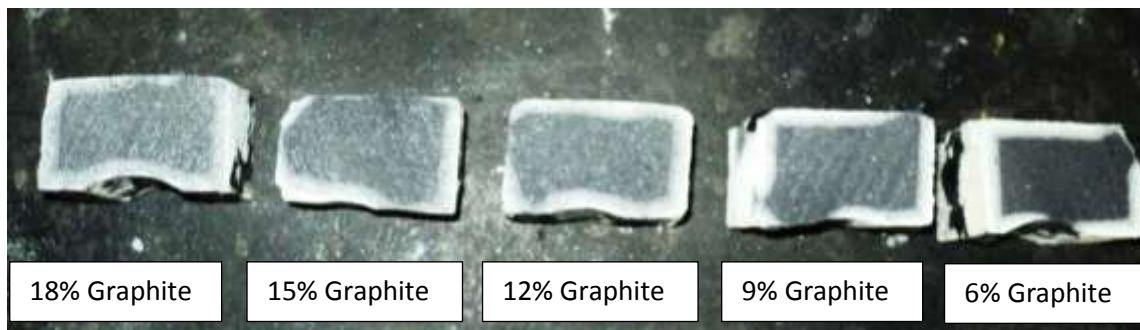


Fig. 5.21 Spalling resistance of Zirconia-Graphite refractory as a function of graphite

Samples with N115 and N220, for all composition did not show any crack up to 15 cycle of thermal shock by water quenching method. It could be correlated with the gap between the aggregates. Both nano carbons had high value of Di butyl phthalate (DBPA). Di butyl phthalate is the ability of the material to form the gap between the aggregate. The increase the gap between the aggregate did not mean to increase in apparent porosity. The increased distance of separation between aggregates were already filled up by nano carbon, therefore it could not affect the apparent porosity. High DBPA means it has high tendency to form a gap between the aggregates. This space between the aggregate helped in decreases the Elasticity of the refractory material. Thereby improvement in the stress relaxation of the refractory can be observed, therefore, the thermal stress in the refractory was less which in turn improved the thermal shock resistance of the zirconia-graphite refractory with inclusion of nano carbon. The variation of the MOE with decrease in graphite percentage is shown in Fig.5.22

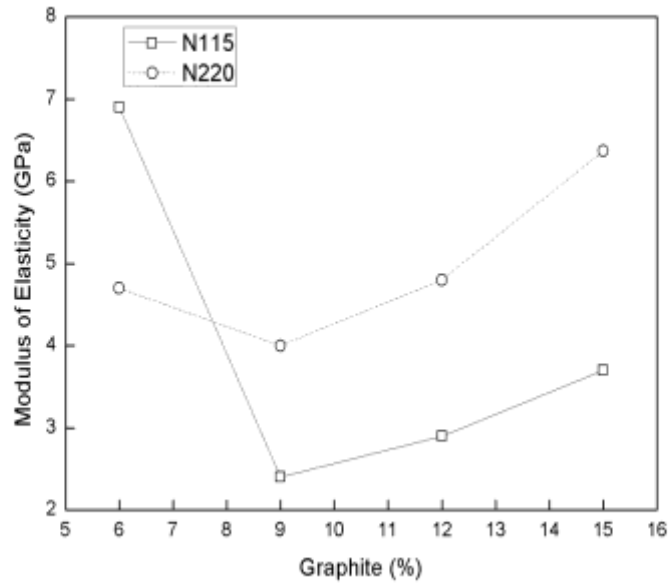
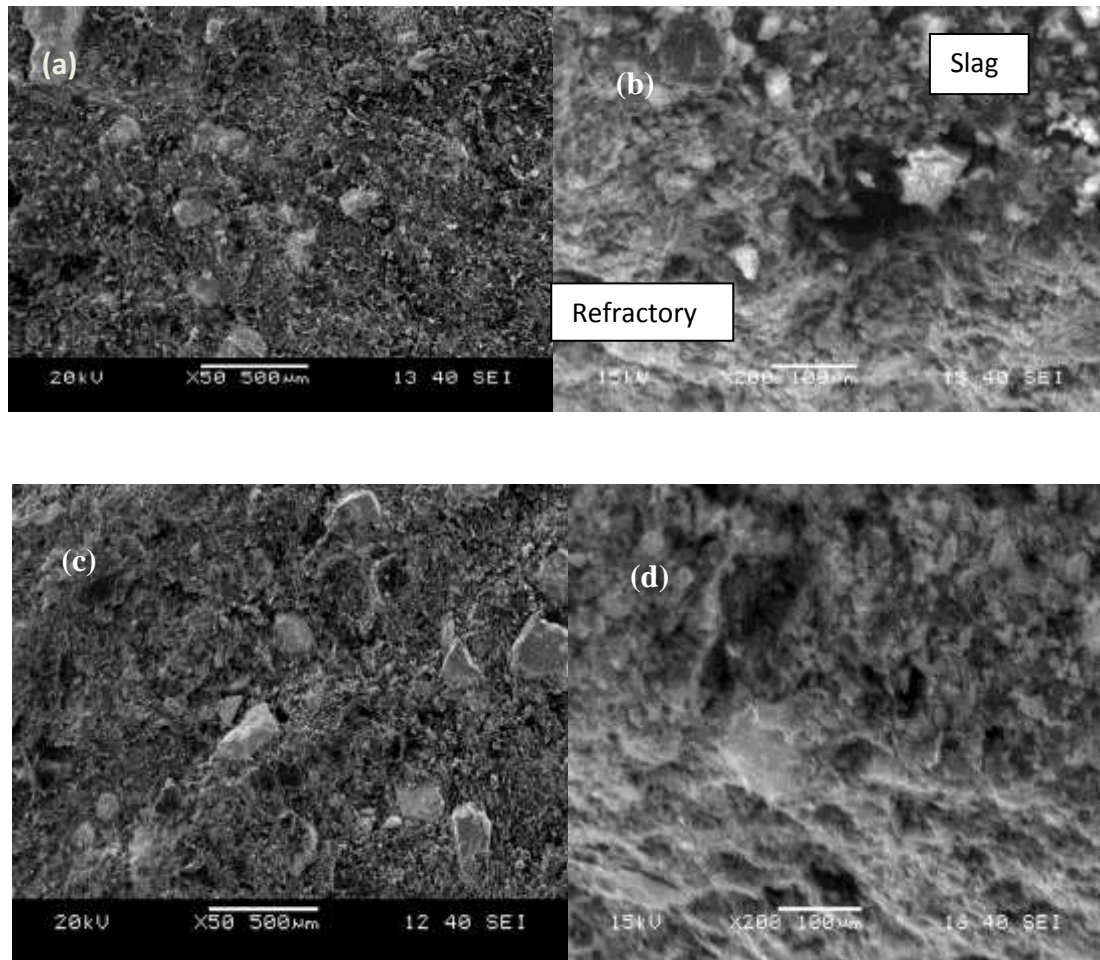


Fig.5.22 Modulus of Elasticity as a function of Graphite content

It could be observed that with the decrease in percentage of graphite from 15% to 9% and inclusion of 0.5wt % N220 nanocarbon, MOE value decreased significantly and after that MOE value increased. The lowest MOE values were observed for sample containing nano carbon N115 for all samples. For samples with 15% and 12% graphite pores were not effectively filled up with nano carbon. As we decreased the percentage of graphite, pores were getting filled by nano carbon hence there was decrease in MOE values. The most effective packing of pores by nano carbon was observed in sample containing 9% graphite. For 9% graphite containing samples more decrease in MOE values were observed for N 115 nano carbon inclusion. It could be due the reason that to N115 had lesser particle diameter than N220 and as the particle diameter became small the gaps between the aggregates were able to accomodate more carbn nano particles, without increasing porosotiy, resulting in lower modulus of elasticity. As the modulus of elasticity of the Zirconia-Graphite refractory decreased, therefore, the thermal spalling resistance resistance has been improved.

Scanning electron Microscope image: The micro structure of zirconia–graphite refractory varying graphite percentage from 15 wt% to 6wt% with inclusion of N115 nano carbon shown is Fig.5.23 An comparison had been shown with sample before corrosion resistance and after corrosion resistance. Refractory phases as well as penetrated slag phases can be clearly distinguished in the mircographs.



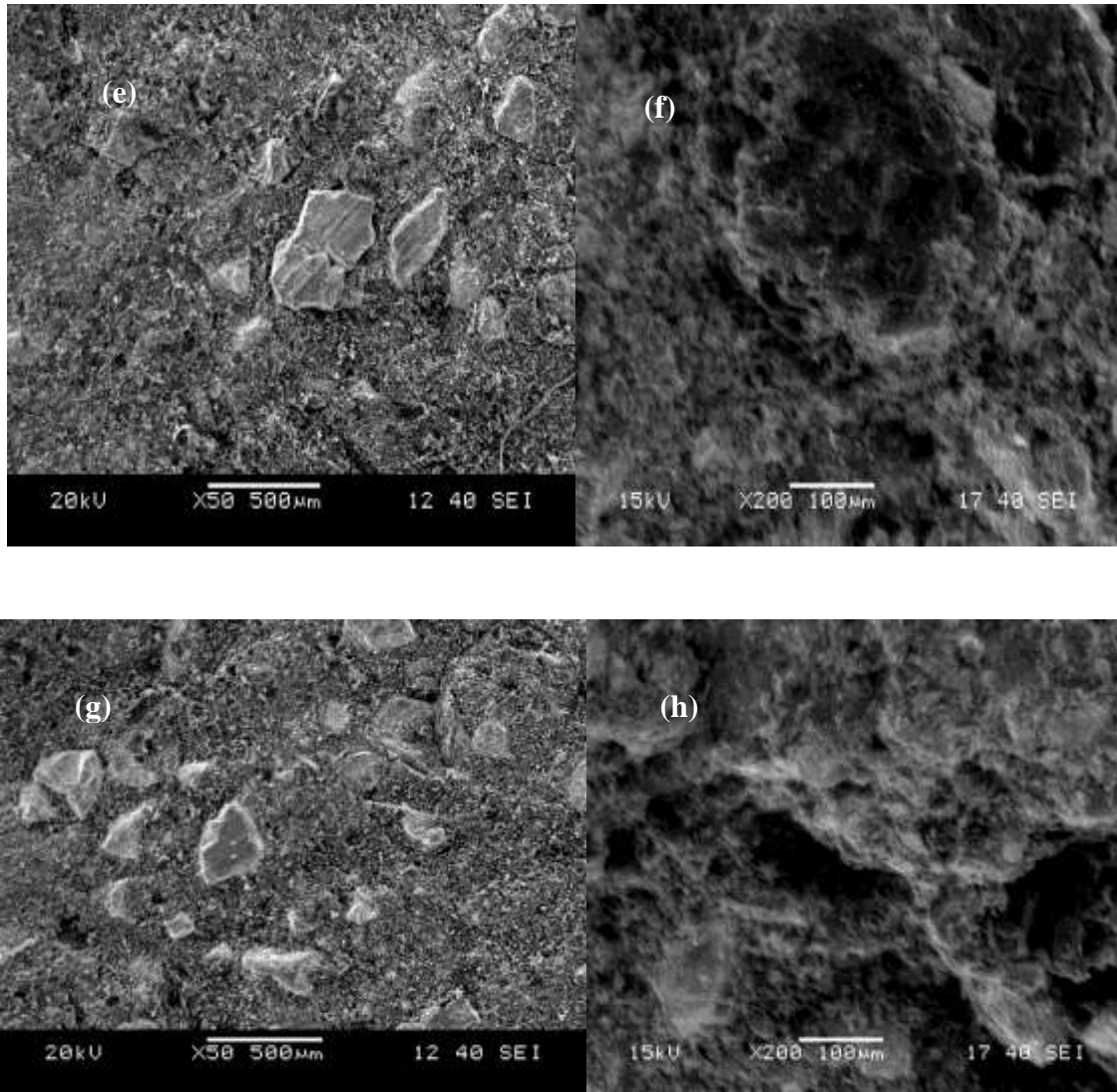


Fig.5.23. SEM image of Zirconia-graphite refractory with (a)15 wt% graphite with 0.5% nano carbon, (b) slag metal interface for 15 wt% graphite with 0.5% nano carbon, (c) 12wt% graphite with 0.5% nano carbon, (d) slag metal interface for 12 wt% graphite with 0.5% nano carbon, (e) 9wt% graphite with 0.5% nano carbon, (f) slag metal interface for 9wt% graphite with 0.5% nano carbon,(g) 6wt% graphite with 0.5% nano carbon, and(h)slag metal interface for 6 wt% graphite with 0.5% nano carbon.

5.3.4.2 Oxidation Resistance

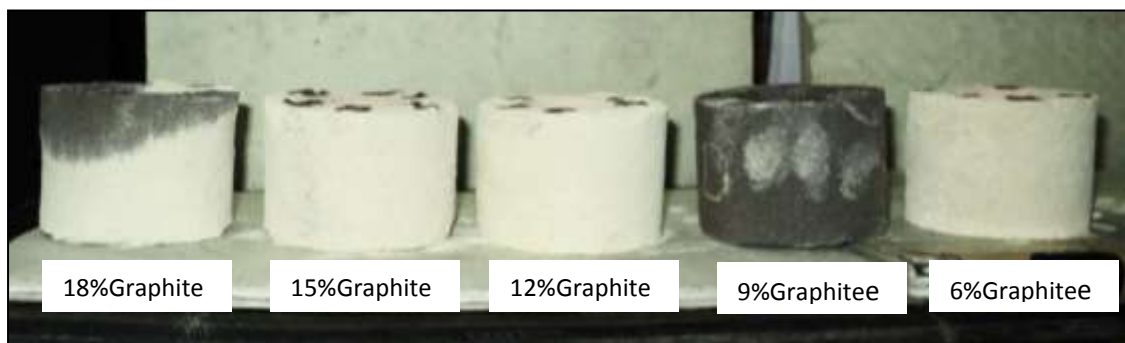


Fig.5.24. Oxidation Resistance test as a function of graphite.

Figure shows the oxidation behaviour of Zirconia-Graphite refractory with decreasing graphite percentage from 15wt% to 6wt% with inclusion of 0.5wt% nano carbon. It has been observed from the figure that Zirconia-Graphite refractory with 9wt% graphite and 0.5wt % nano carbon still retained carbon even after firing at 1200⁰C for 2 hours in an oxidising atmosphere. It could be due to in Zirconia-Graphite refractory with 9 wt% graphite and 0.5wt % nano carbon had filled all the pores of the zirconia matrix. When atmospheric oxygen comes into contact with nano carbon, the nano carbon present in the pores reacts with oxygen and form CO and CO₂. These gases got entrapped inside the pores, hence increasing the gas pressure inside the pores. These enhancements of gas pressure inside the pores can effectively suppress the diffusion of oxygen into the refractories. As a result oxygen would be expected to diffuse only a short distance and the oxidation rate was decreased significantly. Thus refractory containing 9wt% graphite and 0.5wt% nano carbon black had shown enhanced oxidation resistance compared to other [49].

Summary:

Studies on zirconia-graphite refractories by decreasing the percentage of graphite from 15wt% to 6wt% and inclusion of 0.5wt% nano carbon (N115 and N220) has suggested that N115 has better thermo-mechanical properties than N220 for every composition of zirconia-graphite. Also zirconia-graphite refractory with 9wt% graphite and 0.5wt% nano carbon (N115) has shown better thermo-mechanical properties compared to other composition. Further, studies has been done in order to determine the optimum percentage of Nano carbon inclusion on 9wt% graphite containing refractory, so that thermal spalling resistance and slag corrosion resistance can be improved. Therefore, present studies on zirconia-graphite refractories has been prepared with increasing the percentage of nano

carbon (N115) from 0.5wt% to 1.5wt% keeping the graphite percentage fixed to 9wt%. This study had been done in order to determine the optimum nano carbon percentage that can be used with 9wt% graphite, so that the thermal spalling resistance and slag corrosion resistance can be improved.

5.4 Batch formulation of increase in the percentage of nano carbon on 9wt %Graphite in Zirconia-graphite Refractory.

Batch formulation has been done by fixing the graphite percentage to 9wt% in zirconia-graphite refractories. others Raw material used in the formulation of zirconia graphite refractory is same as used in previous section 5.1 The zirconia-graphite refractory has been prepared by increasing the percentage of nano carbon from 0.5wt% to 1.5wt% in 9wt% of graphite. Batch formulation for above study had been shown in table 5.4

Table5.4. Batch formulation of increase in the percentage of nano carbon on 9wt % Graphite in Zirconia-graphite Refractory

Raw Material (wt%)		T-C	T-11	T-12	T-13	T-14
Chemical composition	CaO Stabilized ZrO ₂	82	82	91	91	91
	Graphite(99%FC)	18	18	9	9	9
	Antioxidant	0.5	0.5	0.5	0.5	0.5
	Additives	12	12	12	12	12
	N115	0.0	0.5	0.5	1.0	1.5
Grain Size Distribution of ZrO₂	Coarser	23.8	23.8	26.6	26.6	26.6
	Medium	32.7	32.7	36.5	36.5	36.5
	Fines	25.5	25.5	27.9	27.9	27.9
Apparent Porosity		21.1	22.7	22.7	23.1	24.0
Bulk Density(gm/cc)		3.14	3.07	3.32	3.29	3.21
MOR(Kg/cm ²)		65	62	70	64	60
Width loss(mm)*1		22.38	16.97	13.18	22.30	24.60

*Corrosion resistance test was carried out in Rotary Drum Method with metal and slag [basicity (C/S) = 3], at temperature 1550⁰C±50⁰C, metal and slag were replaced 2 times during one run.

5.4.2 Physical properties of zirconia-graphite refractory by increasing the percentage of Nano Carbon.

5.4.2.1 Apparent Porosity

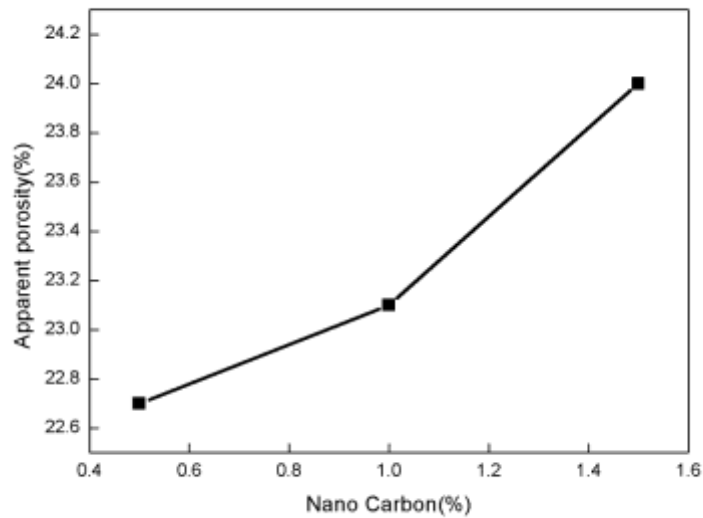


Fig. 5.25 Apparent porosity as a function of Nano carbon

It is seen from the figure that apparent porosity is a function of Nano carbon. It is observed that as the percentage of nano carbon addition to the 9wt% graphite increases from 0.5% to 1.5% apparent porosity is increased from 22.7 to 24.0. It could be due to upto 0.5% nano carbon, pores are almost fill up by the nano carbon. But after 0.5% nano carbon, further filling is not possible, so further increase of nano carbon in the matrix increases the porosity of the ZG refractory.

5.4.2.1 Bulk Density:

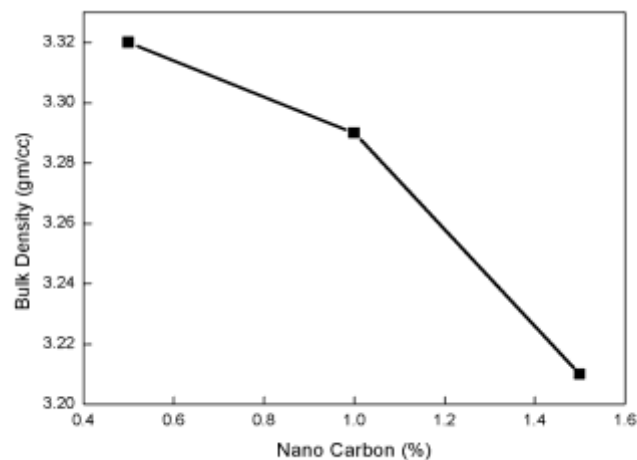


Fig.5.26 Bulk Density as a function of Nano Carbon

It has been observed from the figure that bulk density is a function of nano carbon. It is observed from the figure that as the percentage of nano carbon addition to the 9wt% graphite increases from 0.5% to 1.5% the bulk density decreases from 3.32gm/cc to 3.21 gm/cc. It could be due to the fact that up to 0.5wt% nano carbon, all pores are filled up by the nano carbon and graphite. But after 0.5% nano carbon, further filling is not possible, so further increase of nano carbon in the matrix increases the porosity of the ZG refractory thus resulted in decrease in BD.

5.3.3 Mechanical properties of zirconia-graphite refractory by increasing the percentage of Nano Carbon.

5.3.3.1 Cold modulus of Rupture

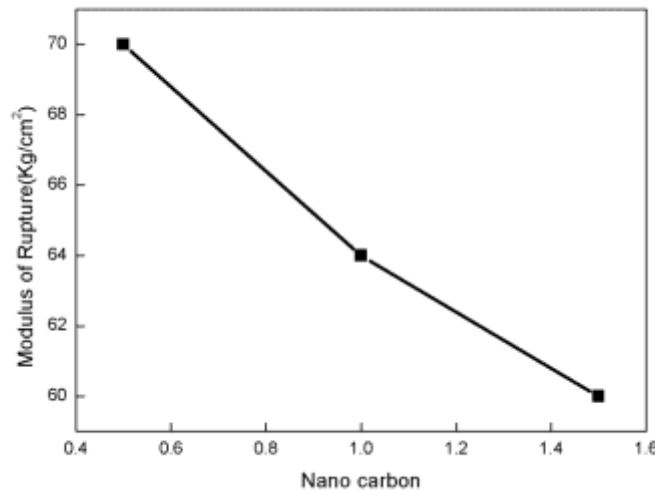


Fig.5.27. Modulus of Rupture as a function of Nano Carbon

It has been observed from the figure that Modulus of rupture is a function of nano carbon addition. It has been observed that as the percentage of nano carbon addition to 9wt% graphite increases from 0.5wt% to 1.5wt % the MOR decreases from 70 MPa to 60MPa. It could be due to increase in the Apparent porosity. As the Apparent Porosity increases the volume of open pores present on the surface increases as the result the bottom surface of the specimen during CMOR testing could not bear the high load and stress generated causes the crack to propagate at the surface resulting in decrease in CMOR.

5.3.4. Thermal properties of zirconia-graphite refractory by increasing the percentage of Nano Carbon.

5.3.4.1 Slag corrosion Index:

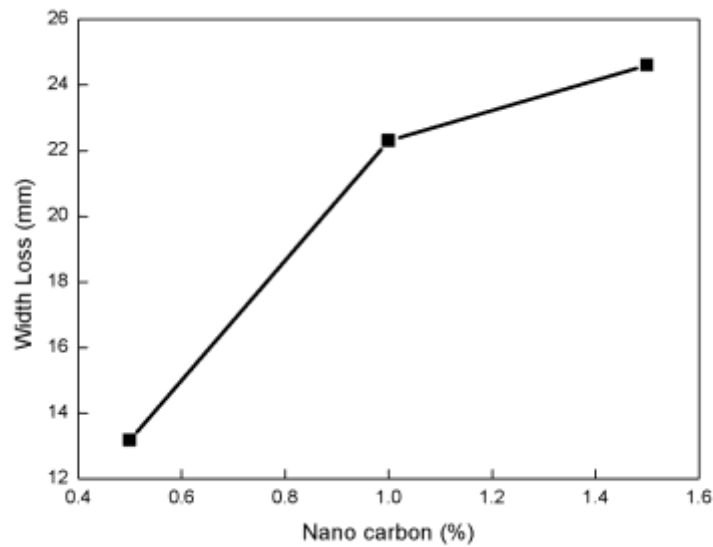


Fig.5.28. Width loss cause due to slag as a function of Nano Carbon

It has been observed from the figure that width loss cause due to slag corrosion is a function of percentage of addition of nano carbon. It is observed that as the percentage of nano carbon present in the 0.9 wt% graphite refractory increase from 0.5 wt % to 1.5wt% the width loss increases from 13.18 mm to 24.60 mm. It could be due to extra nano carbon present on the surface after filling up the pores accumulated the slag inside it voids. Thereby, slag gets more time to be in contact with the refractory surface resulting in corrosion of the refractory surface. Thus slag corrosion resistance was best achieved with 0.5% nano carbon addition to 9wt% graphite.

CONCLUSION

The present work on the fabrication of zirconia-graphite refractory has drawn the following conclusion:

1. Fabrication of zirconia graphite refractory with varying fixed carbon % of graphite

Initial observations had been carried out with the zirconia graphite refractory material, by varying fixed carbon percentage of graphite to 99wt%, 94wt% and 80%. In this, the 99% fixed carbon graphite composition attains lower apparent porosity, higher bulk density, CMOR and low width loss caused by the slag. This 99wt% fixed carbon graphite has lowest free energy, which further leads to less reactive and low wettability of the graphite.

2. Incorporation of Amorphous carbon black replacing 2 wt% of graphite

Then the 2 weight % of amorphous carbon black had been replaced on the 99% & 94 % of fixed carbon containing graphite in zirconia graphite refractory. In this case, apparent porosity, bulk density, CMOR, width loss corrosion due to slag had been deteriorated. This happens due to the higher free energy and more surface area of the amorphous carbon black.

3. Reducing the graphite % and inclusion of 0.5% of N115 and N220 nanocarbon

The next trial had been attempted with the 0.5% of N115 and N220 nanocarbon, by reducing the graphite percentage to 15 wt %, 12 wt %, 9 wt % & 6 wt %. The low apparent porosity, high bulk density, high CMOR and low width loss caused by the slag had been achieved in the composition containing 9 wt % of graphite along with 0.5% for both N115 and N220 nanocarbon. It attains the above said properties due to the higher ability of pore filling of the zirconia matrix. But overall properties had been better with N115 nanocarbon when compared with N220 nanocarbon.

4. Increasing the % of N115 nanocarbon in zirconia graphite refractory

Further with 9 wt % of graphite on the zirconia graphite refractory, the weight percentage of nanocarbon had been tried with 1 and 1.5 wt %. In these cases, the high Apparent porosity, lower Bulk density, low CMOR and high width loss caused by the slag. Since the excess amount of nanocarbon comes on the surface after pore filling, there by deteriorating the overall properties.

9wt % of 99% fixed carbon graphite along with 0.5% Nano carbon (N115) has shown better properties when compared to other combinations tried over here.

REFERENCES

1. European patent.preventon of alumina clogging, 21.09.88,88308760.3
2. Prasad.B..Carbon-Containing Refractories with Antioxidants in Laboratory and Practical application,Refractories World Forum, vol3(August2012): ,pp. 87-93
3. Lee. Y. M. Zirconia Graphite Wear and Steel inclusions, ArcelorMittal Steel Global R&D
4. Sasaki.A. High Performance Nozzle with Inner Bore made of the MgO-C Material, UNITCER, 2-A-3 (2011)
5. Benson. P. M. Liner for submerged Entry nozzle, US5370370 Patent,1994
6. Monaghan.Brian J. Comparative study of oxide inclusion dissolution inCaO-SiO₂-Al₂O₃ slag, iron & Steelmaking,32(3),(2005),pp. 258-264
7. Hongxia. Li.Structure and material design of high performance functional refractories for high-speed continuous casting, UNITCER,2-A-12,(2011)
8. Imaoka.T.Effect of Mold Powder Properties on Corrosion Rate of SEN ZrO₂-C Material.UNITCER,2-A-18,(2011)
9. Lee.S J. Optimisation of Continous Casting Refractory Materials and Designs,UNITCER, vol 2,(1995),pp-95-100.
10. Sen.A. Effect of nano-oxides and anti-oxidants on corrosion and erosion behavior of submerged nozzle for longer sequence casting of steel
11. Daisuke.Y.Improvement of the durability of ZG materials by nano-technology.UNITCER,(2007),pp-349-352
12. Parody. R.Utilization of metallic powders in carbon-containing Refractories,UNITCER,vol- 2 (1987), pp-1051-1059
13. Tamura. S. The Development of the Nano Structural Matrix. UNITCER, 2B-05, (2003)
14. Tamura. S.Technological philosophy and Evolution of Nano-Tech. Refractories, UNITCER 2.00E-16 2011

15. Gardziella.A. Phenolic Resins as Impregnating Agents for Refractories-Present State of Development,UNITCER, vol-2,(1997),pp-975-998
16. Cho. Y.H. Properties of porous PSZ ceramic according to the curing behavior of the phenolic resin with varying relative humidity,Journal of ceramic processing Research,vol-13.No.2, (2012), pp-97-100
17. Sahu. J.K. Effect of Nano-Material on Alumina-Zirconia-Carbon Refractories, UNITCER, vol-2,(2011), pp-223-226
18. Rana.R.P.Effect of nano material addition on the properties of Refractories
19. Matsuo.Y. Effect of the Carbon nanofiber addition on the mechanical Properties of Mgo-C Brick.UNITCER, 2-E-13, (2011),pp-215-218
20. Shiratani.Y. The Application of the Nano Structural Matrix to SN plates,UNITCER, (2005), PDF-134
21. Hattanda.H. The application of Nano-technology to AG material for SN plates and Carbon- Brick for Blast furnace,UNITCER, vol-2,(2011),pp-239-246
22. Gong-Yi Guo.A nearly pure monoclinic nanocrystalline zirconia Journal of Solid State Chemistry VOL-178,(2005) pp-1675-1682
23. TAN Qinghua.Effects of Additives on phase composition, microstructure, and properties of zirconia products fired at different temperatures."China RefractoriesVOL-19.(2010), pp-25-29
24. R Sarkar. Decomposition and Densification Study of Zircon with additives, Interceram,vol-60 pp-308-3011
25. W. LXX.Research on reaction between molten steel and refractories and development of corrosion resistant submerged entry nozzle ,UNITCER,vol-1, (2001),PDF-05
26. M.Ando The Application of Basic materials for CC Refractories. UNITCER,vol-2,(1995),pp-116-124
27. S J lee.Optimisation of Continous Casting Refractory Materials and Designs, UNITCER,vol-2,(1995),pp-95-100
28. Douglas Galesi Blast furnace trough and runners: techniques for minimizing the working lining oxidation process,UNITCER, (2011)108-PDF
29. Li Hongxia.Structure and material design of high performance functional refractories for high-speed continuous casting, UNITCER, (2011),2-A-12

30. Wei Lin. Development of Ladle Shroud and SEN with Heat-insulating Carbon-free Inside Liner,UNITCER,(2011),2-A-16
31. B Prasad. Developmment of composite Anticlogging Nozzles for Continous casting of steel ECCC,vol-13,(2005),pp-450
32. Peng Dejiang,Research on Anti-Oxidization Coating of SEN for Thin Slab Con-Casting,UNITCER(2007), pp-342-344
33. Yasushige Hayashi.An Investigation of Alumina Deposits on the Bore Surface of Submerged nozzles.UNITCER.vol-1,(1987),pp-384-397
34. J.POIRIER .Development of New Submerged nozzles to reduce Alumina Build up in Continous Casting UNITCER,vol-2, (1995),pp-79-86
35. D. B Hoggard.Development of a Liner to Reduce Alumina Build up in graphitized Alumina Submerged Pouring Nozzles used in the Continous Casting of Steel. UNITCER,vol-1(1987),pp-411-424
36. Eishi L ida.Investigation of Anti-alumina Build up material for Submerged Entry Nozzle.UNITCER vol-2,1995,pp-87-94
37. Takuya Imaoka. Effect of Mold Powder Properties on Corrosion Rate of SEN ZrO₂-C Material,UNITCER,(2011),2-A-18
38. Y. VERMEULEN Material Evaluation to Prevent Nozzle Clogging during Continuous Casting of Al Killed Steels,ISIJ International,VOI-42, (2002),pp-1234-1240
39. European patent,prevention of alumina clogging,21.09.88,88308760.3
40. Jouni Ik,heimonen Nozzle clogging prediction in continuous casting of steel "IFAC,15th Triennial World Congress, Barcelona, Spain"(2002)
41. M. Alavanja,"Steelmaking Conf. Proc., Nashville, USA "(1995),pp-415-426
42. A.R. McKague ,Iron Steelmaker ,vol-25 (1998) pp-35-41
43. Gurner. argon injection to protect alumina clogging UK 2111880A,1994
44. Priyadarshi G. Desai, Resin Bonded Liner, US 6475426 B1,(2002)
45. Shinichi Tamura " Carbon Nano Particles-Trends and Hopes for use in Refractories Journal of the Technical Association of Refractories, Japan"30 [4],(2010),pp-275-281
46. R.P.Rana.Effect of nano material addition on the properties of Refractories
47. Brian J. Monaghan.Comparative study of oxide inclusion dissolution inCaO-SiO₂-Al₂O₃iron & Steelmaking slag,vol-32(3),(2005),pp-258-264

48. "Aneziris, C.G, Magnesia-Carbon Brick A high Duty Refractory Material, Interceram,(2003)pp-22-27
49. Mohamad Hassan, The Effect of Nanosized Carbon Black on the Physical and Thermomechanical Properties of $\text{Al}_2\text{O}_3\text{--SiC--SiO}_2\text{--C}$ Composite, Journal of Nanomaterials, (2009), pp-1-5